A STUDY OF TROPOSCATTER PATH LOSS PREDICTION TECHNIQUES

A Thesis Submitted
In Partial Fulfilment of the Requirements
for the Degree of
MASTER OF TECHNOLOGY

By

MAJOR P S. ARORA

to the

DEPARTMENT OF ELECTRICAL ENGINEERING
INDIAN INSTITUTE OF TECHNOLOGY, KANPUR
AUGUST, 1979

CERTIFICATE

This is to certify that the thesis entitled 'A STUDY OF TROPOSCATTER PATH LOSS PREDICTION TECHNIQUES', is a record of work carried out by Major P.S. ARORA under my supervision and that it has not been submitted elsewhere for a degree.

August 7 ,1979

N.C. Mathur

(N.C. MATHUR)
Professor
Department of Electrical Engineering
Indian Institute of Technology
Kanpur

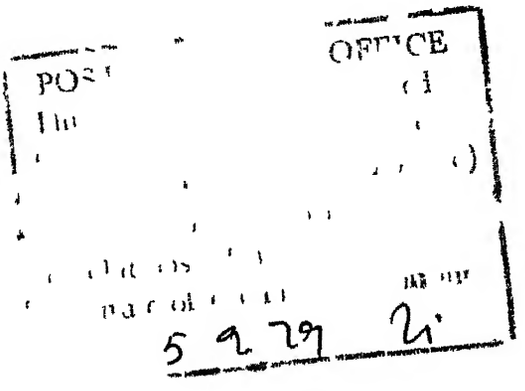

TO MY PARENTS

ACKNOWLEDGEMENT

The successful completion of this work was made possible due to unstinted guidance and valuable suggestions of Dr. N.C. Mathur. I sincerely thank him for his keen interest and supervision which encouraged me to overcome many difficulties encountered in this study. Thanks are also due to Dr. S.C. Majumdar, of Civil Aviation Department, and Dr. S.K. Sarkar of N.P.L., for sparing time and helping me tide over certain difficulties.

I am grateful to my colleague, Major V.K. Girdhar, for helpful discussions and for providing me some very useful data.

I acknowledge the cooperation extended by my wife while I was busy in study and in compilation of this thesis.

I finally thank Mr. J.S. Rawat for his excellent typing.

Kanpur
August, 1979

- Maj. P.S. ARORA

ABSTRACT

The transmission loss between the transmitting and receiving antennas of any troposcatter link determines whether the signal will be received usefully. Currently, a number of techniques, for prediction of path losses on a troposcatter link, are in vogue.

In this thesis, a discussion and inter-comparison between some prominent methods of these has been done, with Kanpur-Nainital troposcatter link data as the base. Studies have also been done to determine the sensitivity of path losses to changes in scatter angle, surface refractivity/ initial refractivity gradient and effective earth radius factor.

Studies have also been done to examine the possibilities of eavesdropping/jamming of troposcatter links, with the eavesdropper/jammer station lying not necessarily within the great circle path of the existing link. One of the prediction methods has been used to predict path losses for eavesdropper/jammer.

TABLE OF CONTENTS

CHAPTER 1

INTRODUCTION

1.1 General

Troposcatter Communication had been developed over the last 20 years into a highly successful and reliable method of communications. It can provide a large number of channels of upto 99.9% reliability between two points as far apart at 600 Kms. However, it is expensive and hence, its use is normally restricted to special applications where other more economical means of communication are either not feasible, or do not provide the same reliability. Some of the typical application areas are

a) Where communication is to be provided over rugged, or inhospitable, terrains and it is not possible to instal repeaters in between, for example, Oceans, Deserts, Mountains etc.

b) Where communication is to be provided across a hostile territory or another political administration.

c) Where communication is required an temporary basis. Transportable troposcatter communication equipment can be used here, for example, communication for mobile formations of the military, or for a mining or oil exploration project in an area detached from headquarters and not affording good communications.

d) Where it is not necessary to drop any channels in between two communication sites. In such circumstances a troposcatter link may be more economical than an LOS chain.

1.2 Requirement for Path Loss Predictions

The transmission loss between the transmitting and receiving antennas of any link determines whether the signal will be received usefully. Each radio system is designed for a maximum allowable transmission loss. Hence, a reasonably accurate prediction of this loss helps in the design, and economics, of the system.

While planning for a troposcatter system, it is essential that we predict the path loss for the link accurately, so that neither the equipment is over designed, nor do we fail to achieve the desired reliability. Pessimistic predictions of path loss are known to have escalated the costs of the system considerably. Prediction of path loss can be done by either carrying out the actual field propagation trials, or by using different prediction techniques with local meteorological data, and geographical and equipment details.

1.3 Existing Methods of Prediction

Currently a number of prediction techniques are in vogue. A discussion on these and intercomparison between

them has been done by Larsen[8] and Sarkar[18]. However, in this thesis only the following have been considered.

1.3.1 NBS 101 Method Given in NBS Technical Note 101[17] and Computer Code[9], it is based on determination of a median reference value of attenuation for unstratified atmospheric conditions, usually corresponding to winter afternoon hours. In this, the reference value has been taken to be a function of N_s, the surface refractivity and contains an empirical adjustment to observed radio data. This method has been rather well documented and is most extensively used, though it is found to be a little pessimistic in predictions.

1.3.2 NPL Method This method, based on a series of observations of propagation mechanisms over the Indian sub continent, is evolved by Majumdar[10,13]. A model of refractive index structure of atmosphere which consists of both, homogeneous and isotropically turbulent medium, and many reflection facets through which the gradient of refractive index is very strong, has been assumed, following Eklund and Wickerts[4]. Hence both scattered and reflected received power has been considered. The meteorological parameter used here is the initial gradient of refractivity, which has been linked to spectral intensity of refractive index fluctuations, C_n^2, (used by Eklund & Wickerts) by an empirical relationship.

1.3.3 CCIR (French Administration) Method Given in Report 238-2, CCIR[1], this method gives basic transmission loss, valid for all climates, based on availability of radio-meteorological parameters, obtained from meteorological soundings. In absence of such data, it permits the use of surface refractivity (N_s) and the gradient between the ground and at 1 Km above the ground (ΔN).

1.3.4 Collins Method This is entirely a graphical method contained in an instruction manual for the U.S. Army[23]. It consists of a series of graphs and nomograms, from which an approximate value of path loss can be determined rather quickly. Interestingly, this method is independent of any radio meteorological parameter. It is good for quick predictions of troposcatter communication by mobile equipment.

1.3.5 Parl's Method A general formula has been evolved by Parl[16], in a recent paper, for basic tropospheric scatter path loss. It encompasses, both, the theory used by NBS 101 and the turbulent scatter theory of Kolmogorov-Obukhov. Either of these two can be used for prediction at a mere switch of the value of the spectrum slope. Further, aperture-to-medium coupling losses can also be determined for various beamwidth, and spectrum slopes. The meteorological

parameters used are variance of refractive index fluctuations and correlation distance of refractive index.

1.4 Statement of the Problem

An experimental troposcatter link was being operated between Nainital and Kanpur with transmitter at Nainital and receiver at IIT, Kanpur. A total of approximately 3600 hours of data has been recorded, covering all the months of the year, evenly as far as possible. Keeping this link in view, the following studies have been carried out.

1.4.1 Inter-comparison between various methods Path loss prediction calculations have been made for this link, using different methods. These results have, then, been compared with the observed path losses to determine the method which predicts values closest to the observed values.

1.4.2 Sensitivity studies Sensitivity of path loss predictions to various essential parameters have been studied for the different methods. The parameters considered are

a) Surface refractivity/Initial gradient of refractivity.

b) Scatter Angle

c) Effective Earth Radius factor

1.4.3 Eavesdropping and Jamming Studies Certain studies have been carried out to determine the path loss to be

encountered by an eavesdropping station, not necessarily in the great circle plane of the operating link, to determine the received signal power for various locations and antenna elevations. In similar vein, path losses to be encountered by a jamming transmitter have also been calculated to determine the required jammer power, for its various locations.

1.5 Scope of the Work

The entire studies of this thesis have been conducted based on radio-meteorological data supplied by National Physical Laboratory (NPL), New Delhi, as given in Radio Refractivity Atlas[12]. The values of N_s have been determined from Mean Surface Refractivity reduced to sea level (N_o), which in turn have been picked up from Majumdar[11]. The other radio-meteorological parameter, Initial Refractivity Gradient (ΔN_1) has been picked up from the Atlas.

The refractivity gradient at 1 Km for use in all methods for calculating the effective earth radius has been taken as initial refractivity gradient, ΔN_i, and not the formula mentioned in NBS 101, as is often done.

The results of these studies are based entirely on a single link (Kanpur-Nainital), and hence may not be adequate for generalization.

The Computer Code[9], for use with NBS 101 method, has not been made use of, because of Note 1 to Report 425-1, CCIR[1], which disqualifies it from use for point-to-point services in the scatter region. Instead our own Fortran IV programme was developed, and used on DEC system 1090.

This work has been divided into various chapters. In Chapter 2 a treatment for finding various parameters of the link and common volume geometry has been given. Since this aspect is common to all methods, it has been treated separately. Also the link parameters and the results of the link-geometry for the Nainital-Kanpur link have been given in brief. The NBS 101 prediction technique has been discussed in Chapter 3. In Chapter 4 the NPL prediction technique has been given with detailed discussion on the Eklund and Wickerts model of received power from turbulent scatter as well as reflection from facets through which refractive index gradient is very strong. Chapter 5 deals with the other prediction methods mentioned above, viz. CCIR (French Administration) method, Collins method and Parl's generalised method. Inter-comparison of various methods with reference to the actually observed median path loss has been given in Chapter 6. Chapter 7 contains a discussion on sensitivity of path

loss to change in certain essential parameters viz. Surface Refractivity/Initial Refractivity gradient, Scatter Angle and Effective Earth Radius. Studies on eavesdropping and jamming of troposcatter links have been dealt with in Chapter 8.

CHAPTER 2

PATH GEOMETRY

2.1 General.

The scatter angle is the most important parameter used in Forward Scatter Loss Calculations. It is defined as the angle between radio horizon rays, in the great circle plane, as determined by the antenna locations. The scatter angle depends on terrain profile, antenna mounting and upon the bending of radio rays in the troposphere. If the heights to be considered are less than one Km above earth's surface, the assumption of constant effective earth radius, a, makes an adequate allowance for ray bending and so the angle can be determined from the terrain profile, by taking radio rays as straight lines.

Since path geometry aspect of prediction of path loss is common to all methods considered, it has been treated separately in this thesis. However, this has already been rather well documented in other works, and so only brief treatment has been given.

For the complete geometry, all heights and distances are in kilometers and angles in radians, unless mentioned specifically.

2.2 Plotting a Great Circle Path

Fig. 2.1 shows the spherical triangle used for computing the great circle path distance between two points, A and B, at the terminals, and where P is the North Pole. Both A and B are in the Northern hemisphere, and latitude ϕ_B of B is higher than latitude ϕ_A of A (only the case of northern hemisphere is considered, being applicable to Indian sub-continent).

The initial bearings, X from terminal A, and Y from terminal B, are measured from True North, and are calculated as follows

$$\tan \frac{Y-X}{2} = \cot \frac{C}{2} \left[(\sin \frac{\phi_B-\phi_A}{2}) / (\cos \frac{\phi_B+\phi_A}{2}) \right]$$

$$\tan \frac{Y+X}{2} = \cot \frac{C}{2} \left[(\cos \frac{\phi_B-\phi_A}{2}) / (\sin \frac{\phi_B+\phi_A}{2}) \right]$$

where C is the difference between the longitudes of two points. The great circle distance Z, is given by

$$\tan \frac{Z}{2} = \tan \frac{\phi_B-\phi_A}{2} \; (\sin \frac{Y+X}{2}) / (\sin \frac{Y-X}{2}) \quad , Z \text{ in degrees.}$$

This is converted to kilometers by

$$d_{km} = 111.18 \; Z^{\circ}$$

2.3 Plotting a Terrain Profile.

Elevations h_1 of the terrain are read from topographical maps and tabulated versus their distance x_1 from the

transmitting antenna. These include successive high and low points along the path. The terrain elevations are modified to include the effect of average curvature of the ray path and earth's surface, so that the profile can be plotted on linear graph paper. The modified elevations y_i of any point h_i, at a distance x_i, from the transmitter along a great circle path, is it's height above a plane horizontal at the transmitting antenna location.

$y_i = h_i - x_i^2/2a$, where a is the effective earth radius, in Kms (determination of 'a' varies for Collin's method., and hence has been treated accordingly).

Fig. 2.2 shows the terrain profile for a transhorizon path.

2.4 Calculation of Effective Antenna Heights

To obtain the effective height of the transmitting antenna, the average height above sea level $\bar{h}_t$ of the central 80% of the terrain between the transmitter and its horizon point is obtained. 31 evenly spaced terrain elevations h_{ti} for $i = 0,1,...30$, where $h_{to} = h_{ts}$ (height above sea level of the ground below the transmitting antenna) and $h_{t30} = h_{Lt}$ (height of radio horizon obstacle above sea level) are determined,

then, $\bar{h}_t = \frac{1}{25} \sum_{i=3}^{27} h_{ti}$

and $h_t = h_{ts} - \bar{h}_t$. Height h_r is similarly defined.

$h_{te} = h_t$, if $h_o \leq 1$ Km

and $h_{re} = h_r$, if $h_r \leq 1$ Km

For antennas higher than 1 Km, a correction Δh_e, as obtained from ray tracing methods described by Bean and Thayer[22] is used to reduce the value h_{te} or h_{re}.

$h_{te} = h_t - \Delta h_e \ (h_t, N_s)$, $h_{re} = h_r - \Delta h_e(h_r, N_s)$

Δh_e can be read from Fig. 6.7, NBS 101[17].

Over a smooth spherical earth with h_{te} and h_{re} less than 1 Km, the following approximate relationship exists between effective antenna heights, and horizon distances (d_{Lt}, d_{Lr})

$$h_{te} = d_{Lt}^2 / 2a \quad , \quad h_{re} = d_{Lr}^2 / 2a$$

2.5 Calculation of Angular Distance, θ

Fig. 2.3 shows the terrain profile with relative distances and angles marked, to aid calculation of the angular distance. Calculations for cases where antenna beams are elevated or directed out of the great circle plane are not dealt with here.

The horizon ray elevation angles θ_{et}, θ_{er} are computed as follows

$$\theta_{et} = \frac{h_{Lt}-h_{ts}}{d_{Lt}} - \frac{d_{Lt}}{2a} \quad , \quad \theta_{er} = \frac{h_{Lr}-h_{rs}}{d_{Lr}} - \frac{d_{Lr}}{2a}$$

where h_{Lt}, h_{Lr} are heights of horizon obstacles, and h_{ts}, h_{rs} are antenna heights, all above mean sea level. As a general rule, the location (h_{Lt}, d_{Lt}) and (h_{Lr}, d_{Lr}) of a horizon obstacle is determined from terrain profile.

At the horizon location, the angular elevation of a horizon ray, θ_{ot} or θ_{or}, is greater than the horizon elevation angle θ_{et} or θ_{er}

$$\theta_{ot} = \theta_{et} + d_{Lt}/a \quad , \quad \theta_{or} = \theta_{er} + d_{Lr}/a$$

If the earth is smooth, θ_{ot} or θ_{or} are zero, and $\theta \simeq Ds/a$, where

$$Ds = d - d_{Lt} - d_{Lr}$$

In the general case of irregular terrain, angles α_{oo} and β_{oo} shown in Fig. 2.3 are calculated as follows

$$\alpha_{oo} = \frac{d}{2a} + \theta_{et} + \frac{h_{ts}-h_{rs}}{d} \quad , \quad \beta_{oo} = \frac{d}{2a} + \theta_{er} + \frac{h_{rs}-h_{ts}}{d}$$

To allow for the effects of a non-linear refractivity gradient, corrections $\Delta\alpha_o$ and $\Delta\beta_o$ are read from Figs. 6.9 and 6.10 of NBS 101 to give α_o and β_o

$$\alpha_o = \alpha_{oo} + \Delta\alpha_o \quad , \quad \beta_o = \beta_{oo} + \Delta\beta_o$$

Now angular distance, $\theta = \alpha_o + \beta_o$ and

path symmetry factor $s = \alpha_o / \beta_o$. The angular distance, θ, is the angle between horizon rays in the great circle plane, and is the minimum scatter angle. $\Delta\alpha_o$, $\Delta\beta_o$ are functions of angles θ_{ot}, θ_{or} and distances d_{st}, d_{sr} defined as

$$d_{st} = d.\beta_{oo}/\theta_{oo} - d_{Lt} \quad , \quad d_{sr} = d.\alpha_{oo}/\theta_{oo} - d_{Lr}$$

For small values of θ_{ot}, θ_{or} and for d_{st}, d_{sr} less than 100 Kms, both $\Delta\alpha_o$, $\Delta\beta_o$ are negligible. Hence,

$$\theta = \theta_{oo} = \alpha_{oo} + \beta_{oo}$$

2.6 Common Volume Geometry

2.6.1 Calculation of common volume An approximate, but useful expression for common volume, also used by Tatarski[19], is obtained below. As shown in Fig. 2.4, the common volume is assumed to be bound by two sets of parallel planes, so that the cross-section of the common volume in the A-Z plane is a rhom-bus. The area of this rhombus is found as follows.

The perpendicular distance AP between the sides AB and CD is given in terms of the beamwidth, γ, and distance of scattering volume from the transmitter, TD (Fig. 2.4) as $AP = TO' \cdot \gamma$

Also, $TO = \frac{TO}{\cos\theta/2} \simeq \frac{D}{2}$

where D is the distance between the Transmitter and the Receiver

Therefore, $AP = \frac{D\gamma}{2}$

Hence, Area ABCD = $AD.AP = \frac{AP^2}{\sin\theta}$

In the Y-direction, the common volume also extends the distance, AP.

Therefore, volume $V = AP \cdot \frac{AP^2}{\sin\theta} = \frac{D^3\gamma^3}{8\sin\theta}$

For θ small, $V \simeq \frac{D^3\gamma^3}{8\theta}$

2.6.2 Extent of common volume In Fig. 2.5, for small value of θ, we can approximate AP to be equal to AC. Hence the extent of common volume will be approximately $h = \frac{D\gamma}{2}$.

2.7 Link Geometry for Kanpur-Nainital Link.

2.7.1 Great Circle Distance

(a) Latitude Kanpur = 29° 21' 38.9"
Nainital = 26° 30' 56"

(b) Longitude Kanpur = 79° 27' 25.6"
Nainital = 80° 14' 10"

(c) Great Circle Distance, d = 325.45 Kms

2.7.2 Calculation of Angular Distance, θ This factor depends on the effective earth radius, a_e, which has been used from different sources for various prediction models.

(a) h_{ts} = 1.8923 Kms , h_{rs} = 0.1458 Kms.

(b) h_{te} = 1.8823 Kms. , h_{re} = 0.1458 Kms.

(c) d_{Lt} = 0.0 Kms. , d_{Lr} = 0.0 Kms.

(d) θ_{et} = 0.0 Kms. , θ_{er} = 0.0 Kms.

(e) θ_{ot} = 0.0 Kms. , θ_{or} = 0.0 Kms.

(f) θ, s

i) a_e = 11021 Kms.

α_{oo} = 0.020 rads , β_{oo} = 0.009 rads

α_o = 0.020 rads , β_o = 0.009 rads

θ = 0.029 rads , s = 2.14

(g) Diagonal width, AC

AC = 2.68 Kms.

2.7.3 Other Details

(a) Antenna Diameter = 28 ft (0.00853 Kms) (Both Transmitter and Receiver).

(b) Frequency of Operation = 2100 MHz.

(c) Waveguide and Coupling Losses = 4 dBs. (Both Transmitter and Receiver)

(d) Transmitter Output Power = 60 dBm.

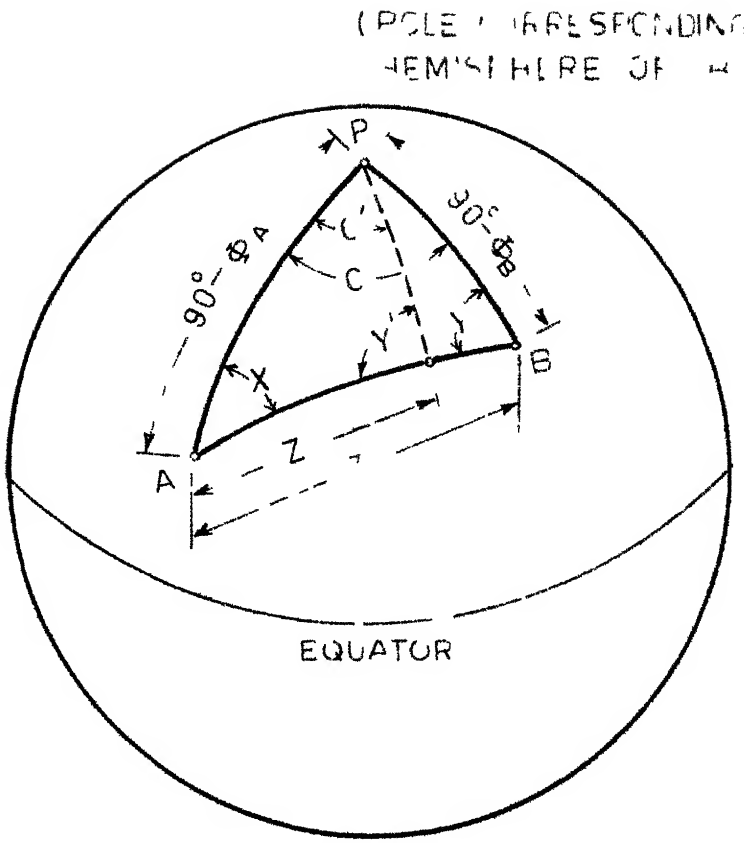

FIG 2 1 SPHERICAL TRIANGLE FOR GREAT CIRCLE PATH COMPUTATIONS

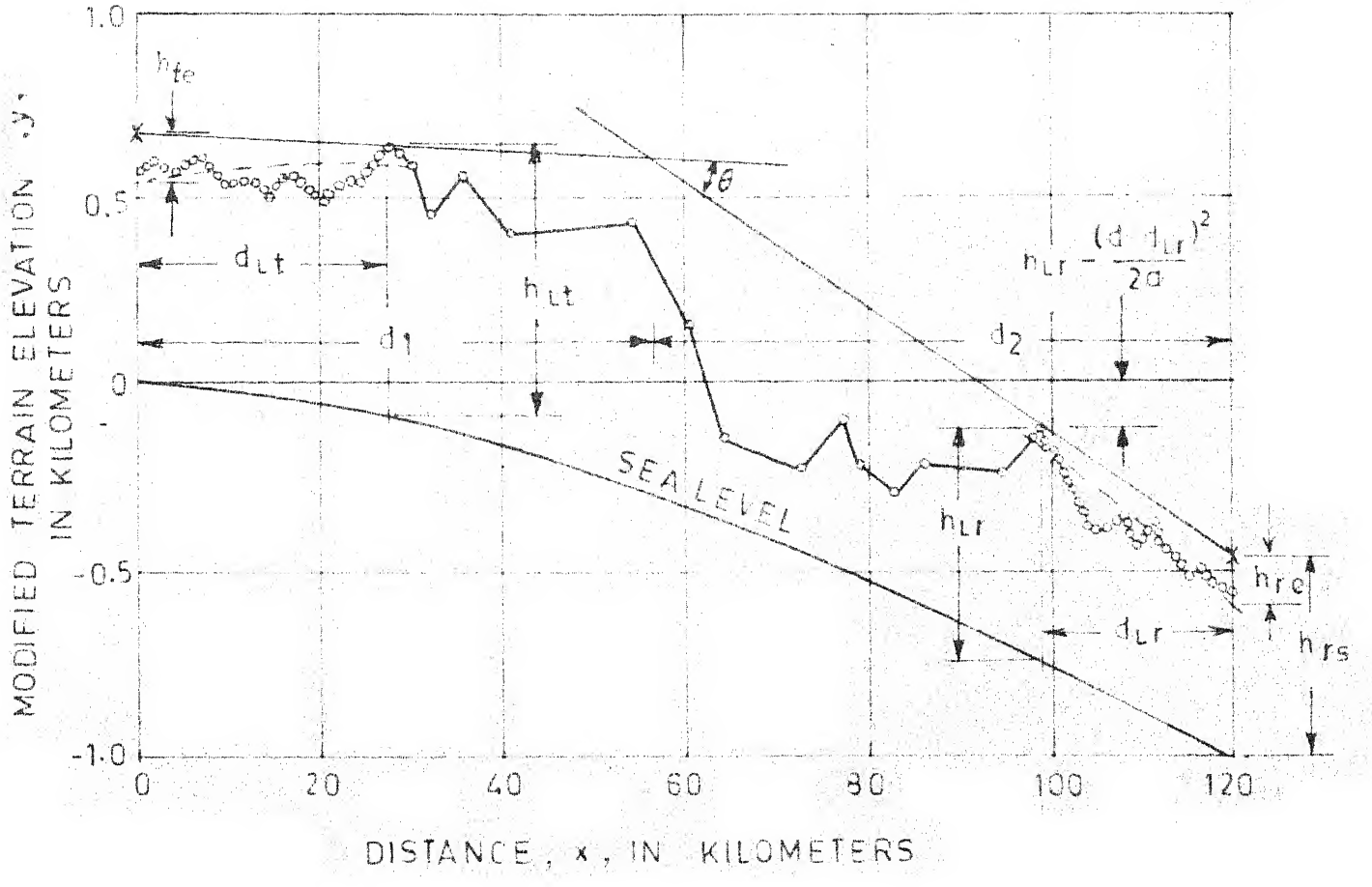

FIG. 2.2 SAMPLE TERRAIN PROFILE FOR A TRANSHORIZON PATH.

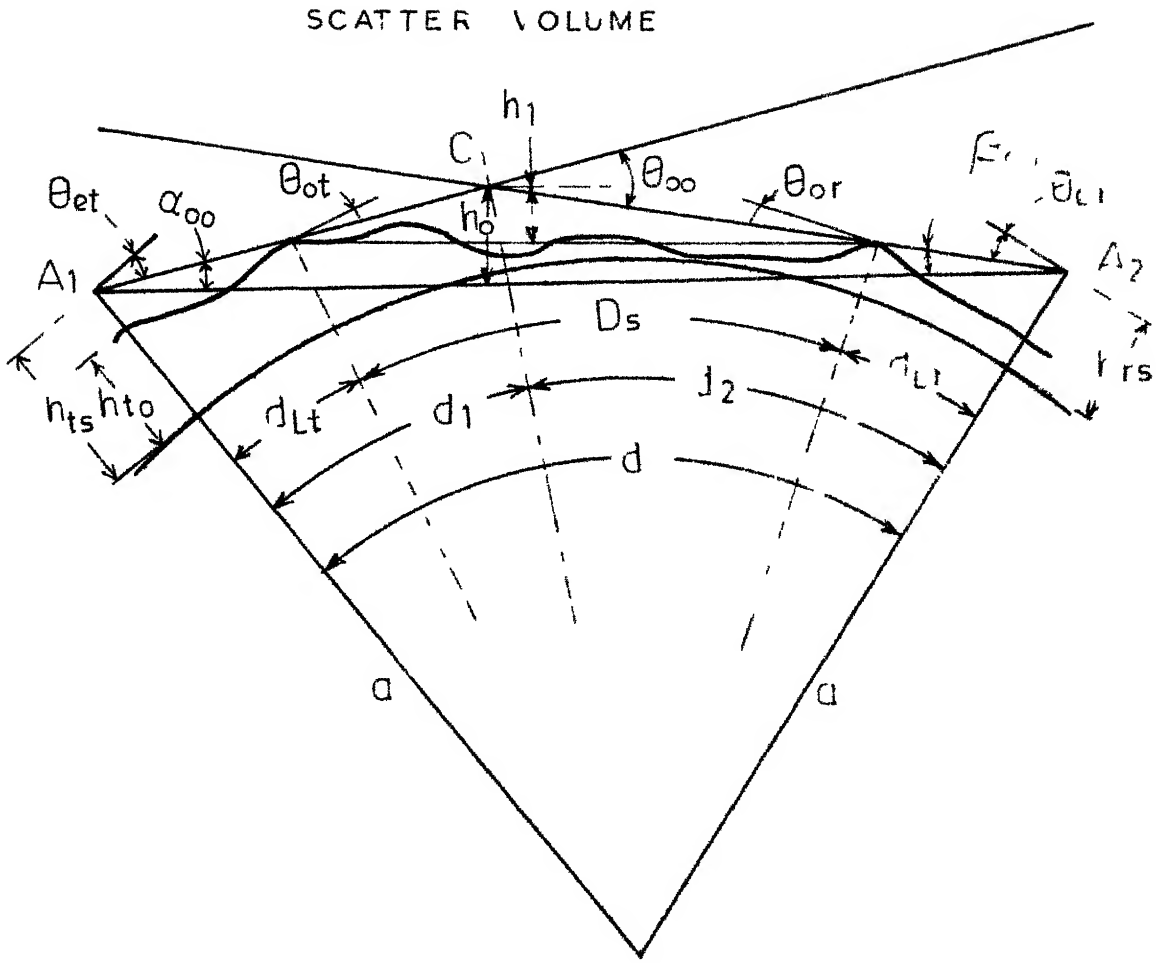

FIG 2 3 SAMPLE PATH GEOMETRY

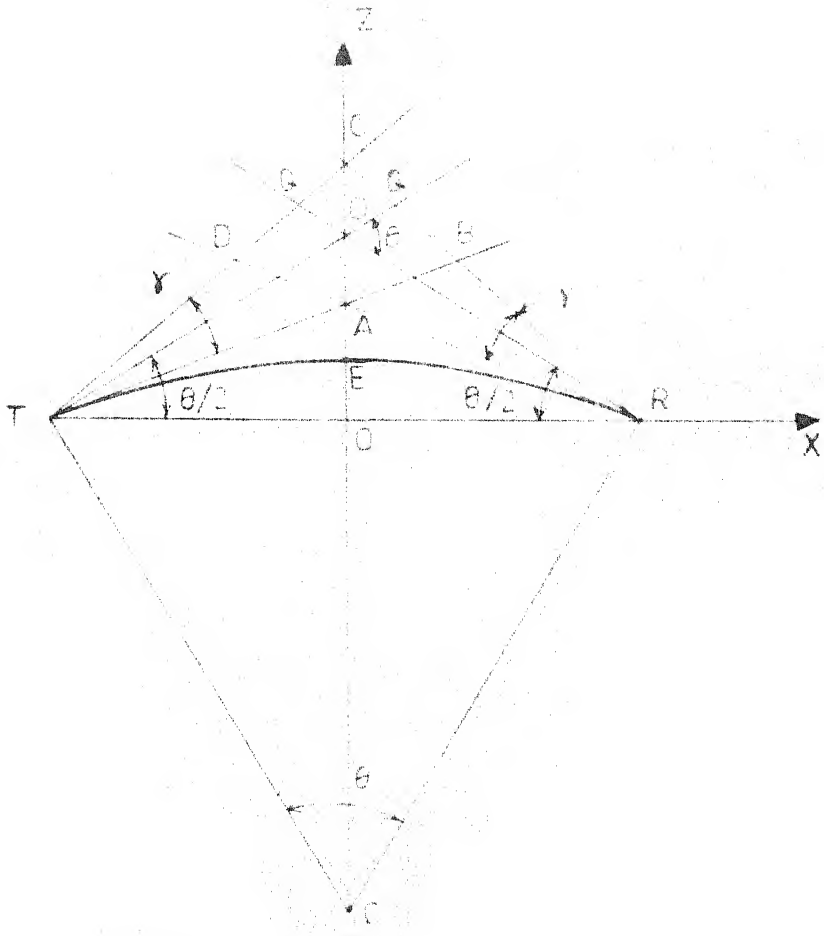

FIG. 2.4 COMMON VOLUME GEOMETRY

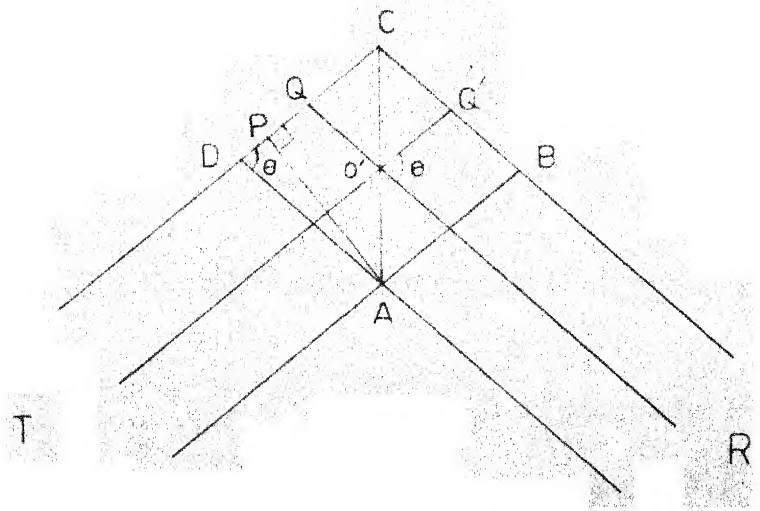

FIG. 2.5 COMMON VOLUME GEOMETRY APPROXIMATED

CHAPTER 3

NBS 101 PREDICTION TECHNIQUES

3.1 General

NBS 101[17] prediction technique for transhorizon communication by forward scatter is the most widely used and accepted method all over the world. It is based on the mathematical model, by Norton et.al. (1964), which gave a vertical wave number spectrum that would achieve agreement between observed radio data and theory of forward scatter from refractivity turbulence. Since it is semi-empirical, no detailed analysis has been done here. The reference value, L_{bsr}, of long-term median basic transmission loss due to forward scatter is given by

$$L_{bsr} = 30 \log f - 20 \log d + F(\theta d) - F_o + H_o + A_a \quad \text{dBs}$$

Where f is the radio frequency in MHz d is the mean sea level arc distance in Kms, θ is the scatter angle, $F(\theta d)$ is a scatter angle dependant attenuation function, F_o is the scattering efficiency term, H_o is the frequency gain function and A_a is the atmospheric absorption.

3.2 Effective Earth Radius.

The bending of radio ray as it passes through the troposphere is dependant on the refractive index gradiant

in the relevant portions. Since we wish to represent radio rays as straight lines, at least within first Km above the surface, an effective earth radius is defined as a function of the refractivity gradient at 1 Km above earth's surface, ΔN_1. Majumdar[10] has correlated ΔN_1 with N_s, based on observations over 13 radiosonde stations in India, and has given the following empirical models for Indian sub-continent.

Inland Areas	$\overline{\Delta N_1} = -3.49 \exp(0.0074\ \bar{N}_s)$
Islands and Southern Coasts	$\overline{\Delta N_1} = -7.12 \exp(0.0054\ \bar{N}_s)$
East Coast	$\overline{\Delta N_1} = -11.53 \exp(0.0039\ \bar{N}_s)$

For West and SE Coast, no relationship could be found. Since effective earth radius is given by

$$a_e = a_o / \left[1 + a_o \frac{\overline{\Delta N}}{10^6}\right], \text{ where } a_o = 6370 \text{ Kms}$$

we have, for Inland Areas, from above

$$a_e = 6370 \left[1 - 0.02224 \exp(0.0074\ \bar{N}_s)\right]^{-1}$$

The Radio Refractivity Atlas[12] gives contours for initial refractivity gradient in N-units/Km. Evaluation of N_1, from the above relationship, for various N_s, over Kanpur-Nainital region was compared with the initial refractivity gradient from the Atlas, and was found to differ greatly. Due to reasons and discussion given in Chapter 6, we reject

the above models by Majumdar. Hence, the effective earth radius should be calculated after reading the mean gradient, ΔN_1, from Atlas, for the region concerned, as follows

$$a_e = 6370 \left[1-6370 \cdot \frac{\Delta N_1}{10^6}\right]^{-1}$$

3.3 The Attenuation Function F(θd)

This function depends upon the most important features of the propagation path, and upon Surface Refractivity, N_s. This includes a small empirical adjustment to data available in the frequency range from 100 to 1000 MHz. For assymetrical paths, the attenuation for a given value of θd (θ in radians and d in Kms) is less than it would be for a symmetrical path. For values of $\theta d \leq 10$, the effect of assymmetry is negligible but increases with increasing (θd), particularly when $s < 0.5$. For values of s between 0.7 and 1.0, the function $F(\theta d)$ for $N_s = 301$ may be computed as follows

for $0.01 \leq \theta d \leq 10$, $F(\theta d)=135.82+0.33\ \theta d+30 \log (\theta d)$

for $10 \leq \theta d \leq 70$, $F(\theta d)=129.5+0.212\ \theta d+37.5 \log (\theta d)$

for $\theta d > 70$, $F(\theta d)=119.2+0.157\ \theta d+45 \log (\theta d)$

For any other values of N_s, the function can be modified by this relationship.

$$F(\theta d, N_s) = F(\theta d, N_s = 301) - \left[0.1(N_s - 301)\ e^{-\theta d/40}\right]$$

For other values of s, Fig. 9.1, NBS 101 can be consulted. If $s > 1.0$, calculations/reading of graphs must be based on $\frac{1}{s}$.

3.4 Frequency Gain Function, H_o

If antennas are considered sufficiently high, the ground reflected energy doubles the incident power on scatterers visible to both antennas, hence increasing the power scattered to the receiver. As the frequency is reduced, effective antenna height, h_{te}/λ or h_{re}/λ in wavelengths, become smaller, and ground reflected energy tends to cancel direct-ray energy at the lower part of the common volume, where scattering efficiency is greatest. This function is distance dependant, decreasing rapidly with increasing distance, till it approaches a constant value.

For $h_{te}/\lambda > 4$ a/d and $h_{re}/\lambda > 4$ a/d, H_o is negligible. H_o is known to vary with a parameter ηs which is defined as

$$\eta s = 0.5696\, h_o \left[1+(0.03-2.32N_s x10^{-3}+5.67N_s^2 x10^{-6}) \exp(-3.8h_o^6\, x10^{-6})\right]$$

$$h_o = sd\theta/(1+s)^2 \text{ Km.}$$

Parameters r_1 and r_2 are defined as

$$r_1 = 4\pi\theta\, h_{te}/\lambda \quad , \quad r_2 = 4\pi\theta\, h_{re}/\lambda$$

where h_{te}, λ are in Kms, and θ in radians.

3.4.1 Case I - $\eta s \geq 1.0$ Functions $H_o(r_1)$ and $H_o(r_2)$ are read from Fig. 9.3, NBS 101. Then H_o is given by

$$H_o = \left[H_o(r_1)+H_o(r_2)\right]/2 + \Delta H_o$$

where, $\Delta H_o = 6(0.6 - \log \eta_s) \log s \log q$

where, $s = \alpha_o/\beta_o$ and $q = r_2/sr_1$.

If $\eta_s > 5$, value of H_o for $\eta_s = 5$ is taken

If $s > 10$ or $q > 10$, use $s = 10$ or $q = 10$

If $s < 0.1$ or $q < 0.1$, use $s = 0.1$ or $q = 0.1$

If $\Delta H_o \gg \left[H_o(r_1)+H_o(r_2)\right]/2$, use $H_o = H_o(r_1)+H_o(r_2)$

If ΔH_o would make H_o negative, use $H_o = 0$

3.4.2 Case II - $\eta_s < 1.0$ First obtain H_o for $\eta_s = 1$ as per Case I, and then compute $H_o(\eta_s = 0)$ as follows.

3.4.2.1 $h_{re} \neq h_{te}$

$$H_o(\eta_s=0) = 10 \log\left[\frac{2(1-h_{re}^2/h_{te}^2)}{r_2^2 \; h(r_1)-h(r_2)} \right]$$

where, $h(r_1)=r_1 \cdot f(r_1)$; $f(r_1)= C_i(r_1) \sin r_1 + \left[\pi/2-S_i(r_1)\right]\cos r_1$,

$h(r_2)=r_2 \cdot f(r_2)$, $f(r_2)= C_i(r_2)\sin r_2 + \left[\pi/2-S_i(r_2)\right]\cos r_2$,

$$C_i(r) = \int_{\infty}^{r} \frac{\cos t}{t}\, dt \; ; \; S_i(r) = \int_{\infty}^{r} \frac{\sin t}{t}\, dt$$

3.4.2.2 $h_{re} = h_{te}$

$$H_o(\eta_s=0)= 10 \log\left[\frac{4}{r^2 \left[h(r)-rg(r) \right]} \right]$$

where, $g(r) = C_i(r) \cos r - \left[\pi/2 - S_i(r)\right] \sin r$

Now, $H_o(\eta_s<1)= H_o(\eta_s=0)+\eta_s \left[H_o(\eta_s=1)-H_o(\eta_s=0)\right]$

H_o rarely exceeds 25 dBs, except for very low antennas.

3.5 Scattering Efficiency Term, F_o

This term allows for reduction in scattering efficiency at great heights in the atmosphere.

$$F_o = 1.086 \; (\eta_s/h_o)(h_o-h_1-h_{Lt}-h_{Lr}) \quad \text{dB}$$

where, $h_o = sd\theta \,/(1+s)^2$ Kms, $h_1 = sD_s \, \theta/(1+s)^2$

where, $D_s = d - d_{Lt} - d_{Lr}$

This correction term rarely exceeds 2 dB.

3.6 Functions V (0.5,d_e) and Y (q, d_e).

To cater for long term power fading, NBS 101 divides the world into 8 climatic regions (Northern plains of India would be covered under 'Continental Temporate'). Median values of data available have been related to long term reference value, L_{bsr}, by a parameter V(0.5,d_e), where d_e is the effective distance and is defined as follows

$$d_{s1} = 65\ (100/f)^{\frac{1}{3}}\ \text{Km},\quad d_L = \sqrt[3]{2h_{te}} + \sqrt[3]{2h_{re}}\ \text{Km}$$

where h_{te}, h_{re} are in meters and f in MHz.

For $d \leq d_L + d_{s1}$, $\quad d_e = 130\ d/(d_L+d_{s1})$ Km

For $d > d_L + d_{s1}$, $\quad d_e = 130+d - (d_L+d_{s1})$ Km

Then, predicted long-term transmission loss exceeded by half of all hourly medians, for a given climatic region, L(0.5), is given by

$$L(0.5) = L_{bsr} - V(0.5,d_e) \quad \text{dB}$$

V(0.5,d_e) is given in Fig. 10.13, NBS 101, for different climates as a function of d_e. Alternately, this function can also be calculated from expressions given in Appx. III.7 and constants in table III.5, NBS 101. Different climatic regions have been treated separately.

A method for calculating transmission loss not exceeded for a fraction 'q' of hourly medians for a specified climatic region is

$$L(q) = L(0.5) - Y\ (q,\ d_e) \quad dB$$

where $L(q,d_e)$ is the variability of L(q), relative to its long-term median value L(0.5). Hence, for a given climatic region, the cumulative distribution of transmission loss can be obtained. Expressions are given in Appx III.7 and constants in table III.6, III.7, NBS 101 for different climatic regions.

Long-term power fading aspect of prediction of path loss for climates other than 'Continental Temperate', in NBS 101, is based on very scanty data and so may not be very reliable.

CHAPTER 4

NPL PREDICTION TECHNIQUE

4.1 General.

Majumdar[10,13] has evolved a method of prediction of long term median value of transmission loss over transhorizon tropospheric propagation paths in India, as a result of extensive radio wave propagation and radio-meteorological studies in five different regions of the country. He has correlated the long term signal strength at 120 MHz and 2 GHz with surface refractivity, N_s and refractivity gradient at various levels. The correlation coefficient with initial refractivity gradient, ΔN_1 (across a nominal altitude interval of 250 m above surface) was found to be the highest for all paths. Also the slopes of regression lines were found to be different for different regions of ΔN_1, indicating different propagation mechanisms. Correlation of signal strength with N_s was particularly found to be poor. This ΔN_1 has, then, been linked up with parameter C_n^2 (spectral intensity of refractive index fluctuations) in Eklund and Wickerts[4] model for tropospheric propagation through scatter as well as reflection. The transmission loss is actually calculated using this method. Effects of super refraction during high gradient conditions, have also been taken into account by Majumdar, while calculating the received power due to reflection.

4.2 Eklund and Wickerts Scatter and Reflection Model

4.2.1 General Eklund and Wickerts[4] have evolved a model for calculation of received power under the assumption that tropospheric refractive index field of the common volume is of a turbulent structure (variations obeying -5/3 spectral law), and also that there are a number of locally sharp boundaries, within this volume, which act as reflecting facets. An empirical relationship between intensity of turbulence and refractive index gradient through the reflecting facets has also been expounded by them, based on certain meteorological measurements. It is claimed that this theoretical prediction of expected signal power is in good agreement with the experimental results.

4.2.2 Model of Refractive Index Field

Airborne refractometer measurements indicated that refractive index variations in troposphere obey the -5/3 spectral law with variations of 'spikes' of refractive index over small distances (horizontal and vertical, both). Again, airborne measurements of refractive index at altitudes upto 3000 m indicated that atmosphere contains volumes of excess refractive index, with sharp boundaries. Based on above, a model for refractive index field of atmosphere was evolved, so that the received signal power, P_R, is a

sum of received signal power due to scattering by a homogeneously and isotropically turbulent medium (P_S) and power due to reflection by many small facets through which the refractive index gradient is very strong (P_D).

Since simultaneous direct measurements of refractive index along with radio measurements were not available, the model has been developed using meteorological knowledge of atmosphere. The mechanisms which cause sharply bounded volumes of air of excessive humidity are known to be

(a) Thermal Convection. Here the volumes of excessive humidity are like spherical bubbles.

(b) Reduced vertical exchange of humidity due to thermal stability. This is encountered mostly along with inversion layers. Gravity waves or shear zones (in vicinity) will create isolated volumes having sharp boundaries.

Interaction between wet and dry air causes refractive index fluctuations, and so through this turbulence the strong gradients will be broken down into a spectrum of fluctuations obeying the -5/3 spectral law. This gives rise to a relationship between refractive index gradient (Δn) and spectral intensity of refractive index fluctuations (C_n^2). Eklund and Wickerts have presumed a linear relationship, picking the constant from maximum of observed values of Δn and C_n^2 from the most effective part of the common volume.

$$\Delta n = 0.6\, C_n^2 \times 10^{10} \qquad (4.1)$$

The meteorological parameters of significance towards calculation of P_D are Δn, C_n^2, shapes of volumes of excessive refractive index, number of such volumes in the common volume, and thickness of boundaries of such volumes. Of these, only Δn and C_n^2 have been taken as variable parameters, being the most significant, and the others are considered constants. The boundaries of all such volumes are considered to be curved with radius, R = 1000 m (a value chosen to represent both the mechanisms of formation of such volumes, mentioned above). The thickness of the boundaries, B, is considered to be 3 m, and their numbers (estimated from airborne refractometer measurements and angel studies) as $N = 10^{-7}$ per m^3 at 1000 m height, and $N = 10^{-9}$ per m^3 at 2000 m height.

4.2.3 Calculation of Power Reflection Coefficient, $|R_o|^2$ The following result has been obtained, in different forms, by Friis et.al.[5], DuCastel[3], Walt[25] and Thayer[21].

$$\text{reflection coefficient, } r = \frac{1}{2\cos^2 I} \int_{z_2}^{z_1} \frac{d}{dz}(n(z)).e^{-j2k(\cos I)z}\, dz$$

where, I = angle of incidence at the reflecting layer,

$k = 2\pi/\lambda$,

and $z_2 > z_1$, z being the vertical coordinate.

This formula neglects all internal reflections within a layer, and uses not the total change Δn in the layer, but its gradient.

Eklund and Wickerts[4] have defined the refractive index profile through the boundary by two exponential functions

$$n(z) = n_o + \frac{\Delta n}{2}\left(1 - e^{\frac{2}{z_o}\cdot z}\right), \quad z < 0 \qquad (4.3a)$$

and $$n(z) = n_o + \frac{\Delta n}{2}\left(1 - e^{-\frac{2}{z_o}\cdot z}\right), \quad z > 0 \qquad (4.3b)$$

where $2z_o = B$, the layer thickness.

Taking derivatives,

$$\frac{dn(z)}{dz} = -2\frac{\Delta n}{B} \cdot e^{\frac{4z}{B}}, \quad z < 0 \qquad (4.4a)$$

and $$\frac{dn(z)}{dz} = -2\frac{\Delta n}{B} \cdot e^{\frac{-4z}{B}}, \quad z > 0 \qquad (4.4b)$$

Defining an effective layer thickness, (DuCastel[3])

$$\chi = KB \cos I$$
$$= KB \sin\psi, \quad \psi = \text{grazing angle}$$
$$\text{or } \chi \cong KB\psi, \quad \text{since } \psi \text{ small} \qquad (4.5)$$

Also defining a normalized height variable, y

$$y = \frac{z}{B} \simeq \frac{K\psi z}{\chi} \qquad (4.6)$$

Now, (4.2) becomes

$$= \frac{1}{2\psi^2} \int_{\infty}^{0} \frac{-2\Delta n}{B} \; e^{\frac{-4}{B} By} \cdot e^{-j2\chi y} \cdot B \; dy + \frac{1}{2\psi^2} \int_{0}^{-\infty} \frac{-2\Delta n}{B} \cdot e^{\frac{+4}{B} By} \cdot e^{-j2\psi y} \cdot B \; dy$$

$$= \frac{-\Delta n}{\psi^2} \left[\int_{\infty}^{0} e^{-(4+j2\chi)y} \cdot dy + \int_{0}^{-\infty} e^{(4-j2\chi)y} \cdot dy \right]$$

$$= \frac{-\Delta n}{2\psi^2} \left[\frac{-1}{2-j\chi} + \frac{-1}{2+j\chi} \right]$$

$$= \frac{\Delta n}{2\psi^2} \; \frac{4}{4+\chi^2} = \frac{\Delta n}{2\psi^2} \left[\frac{1}{1+(\frac{\chi}{2})^2} \right]$$

substituting back for χ ,

$$r = \frac{\Delta n}{2\psi^2} \left[\frac{1}{1+(\frac{2\pi}{\lambda} \cdot \frac{B.\psi}{2})^2} \right] \tag{4.7}$$

Power reflection coefficient

$$|R_o|^2 = \frac{\Delta n^2}{4\psi^4 \left[1+(\frac{\pi B \psi}{\lambda})^2 \right]^2} \tag{4.8}$$

4.2.4 Prediction of Received Power due to Scattering If d be the distance between the transmitter and the receiver, P_T, the transmitter power, G_T, the transmit antenna gain, then at the receiver antenna the free space power density is given by

$$P_{FS} = \frac{G_T P_T}{4 \pi d^2} \qquad (4.9)$$

Assuming the scattering volume to be located at a distance d/2 from the transmitter antenna, the power density here would be

$$P_1 = \frac{4 G_T P_T}{4 \pi d^2}$$

The amount of power scattered in solid angle Ω will be $P_1 \sigma$, where σ is the effective cross section for scattering corresponding to illumination by solid angle Ω.

At the receiving antenna i.e. at distance d/2 from the scattering volume, this power is distributed over an area $(d/2)^2 \Omega$. Hence power density, at receiver antenna, of scattered energy, P_S will be

$$P_S = \frac{4 P_T G_T}{4 \pi d^2} \cdot \sigma \cdot \frac{4}{d^2 \Omega}$$

Therefore,

$$\frac{P_S}{P_{FS}} = \frac{4 P_T G_T}{\pi d^2 \Omega} \cdot \frac{4 \pi d^2}{P_T G_T}$$

$$= \frac{16 \sigma}{d^2 \Omega} \qquad (4.10)$$

Effective cross section, σ, is defined by Tatarski[19] as a function of scatter angle, θ, as only a small group of

spectral components of the turbulence participate in the scattering, at a given angle, θ. Tatarski's equation 4.45 gives σ^+ as

$$\sigma = 2\pi K^4 \quad \phi_n(2K \sin \theta/2) V \sin^2(\chi) \Omega \qquad (4.11)$$

where $K = \frac{2\pi}{\lambda}$, V is the volume of turbulent medium, χ is the angle between unit vector directed from scatter volume to receiving antenna and electric vector of the incident ray. Normally $\chi \simeq \frac{\pi}{2} + \theta$. $\phi_n(2K \sin \theta/2)$ is the wavenumber spectrum, or the spectral density, and is given by Tatarski[19] equation 4.44 as

$$\phi_n (2K \sin \theta/2) \simeq 0.033 \, C_n^2 \, K^{-11/3} \, \theta^{-11/3} \text{(for small } \theta) \qquad (4.12)$$

V is the size of the scattering volume. For narrow beam antennas it can be approximated by

$V \simeq \frac{d^3 \gamma^3}{8\theta}$, where γ is the effective angular beamwidth of the antenna. (For this approximation, refer to Section 2.6.1).

Now 4.10 becomes

$$\frac{P_S}{P_{FS}} = \frac{16}{d^2 \Omega} 2\pi K^4 \sin^2 \chi \quad \frac{d^3 \gamma^3}{8\theta} \phi_n(2K \sin \theta/2) \Omega$$

$$= 4\pi K^4 \sin^2 \chi \, \gamma^3 \, \phi_n (2K \sin \theta/2) \frac{d}{\theta} \qquad (4.13)$$

For a smooth earth case, and for antenna pointing horizontally,

$\frac{d}{\theta} = a_e$ (effective radius of the earth)

and for small θ, we get $\sin^2 \chi \simeq 1$

substituting 4.12 in 4.13, we get

$$\frac{P_S}{P_{FS}} = 0.76\, C_n^2\, a_e\, \lambda^{-1/3}\, \gamma^3\, \theta^{-11/3} \quad \left[\because K = \frac{2\pi}{\lambda}\right] \tag{4.14}$$

Modulus of refractivity, M, is defined as

$$M \triangleq \left[(n-1) + \frac{h}{a}\right] \times 10^6$$

Therefore, gradient of refractive modulus

$$\frac{dM}{dh} = \left(\frac{dn}{dh} + \frac{1}{a}\right) \times 10^6 \tag{4.15}$$

Effective earth radius, $a_e = \dfrac{a}{1+a\frac{dn}{dh}}$

$$\text{or} \quad a_e = \frac{a}{1+a\frac{dM}{dh} \times 10^{-6} - \frac{1}{a}} \tag{4.16}$$

Substituting for a_e in 4.14, we get

$$\frac{P_S}{P_{FS}} = 0.76\, C_n^2\, \frac{10^6}{\frac{dM}{dh}}\, \lambda^{-1/3}\, \gamma^3\, \left(\frac{d}{10^6} \cdot \frac{dM}{dh}\right)^{-11/3} \quad [\text{as } \theta = d a_e]$$

$$\text{or } \frac{P_S}{P_{FS}} = 0.76 \times 10^{28}\, C_n^2 \left(\frac{dM}{dh}\right)^{-14/3} d^{-11/3}\, \lambda^{-1/3}\, \gamma^3 \tag{4.17}$$

4.2.5 Prediction of Received Power due to Reflection Assuming that (a) The troposphere is completely mixed, but for reflecting surfaces set up by volumes and curved facets, and (b) Geometrical

area, S, of reflecting surface is small compared to First Fresnal Zone dimensions, but large compared to the wavelength. Following Friis et.al[5] ,the following method for finding the bistatic radar reflection area is found.

Fig. 4.1 gives the approximate geometry for reflection. The effective dimensions of the layer will be those projected normally to the direction of propagation. Hence size, S, will be

$$S = c \cdot b\psi \quad (\text{as } \psi \text{ is small})$$

The received power, in terms of Fresnal integrals, will be

$$P_D = \frac{P_T G_T}{4\pi(d/2)^2} A_R \left[C^2(u)+S^2(u)\right]\left[C^2(v)+S^2(v)\right] \cdot |R_o|^2$$

('Radar' formula of Friis et.al.[5])

since $G_T = \frac{4\pi A_T}{2}$,

$$P_D = \frac{P_T A_T A_R}{\lambda^2 . d^2/4} \left[C^2(u)+S^2(u)\right]\left[C^2(v)+S^2(v)\right] \cdot |R_o|^2 \qquad (4.18)$$

where C(x) and S(x) are the Fresnal Integrals, and

$$u = \frac{c}{\sqrt{\lambda d/2}} , \quad v = \frac{b}{\sqrt{\lambda d/2}} , \quad C(x) = \int_o^x \cos t^2 \, dt, \quad S(x) = \int_o^x \sin t^2 dt$$

When both u and v are very small, we have approximately,

$$C(u) = u \quad , \quad C(v) = v$$

$$S(u) = 0 \quad , \quad S(v) = 0$$

Therefore, $P_D = \frac{P_T A_T A_R}{\lambda^2 d^2} \cdot 4 \cdot \frac{c^2}{\lambda d/2} \cdot \frac{b^2 \psi^2}{\lambda d/2} \cdot |R_o|^2$

$$= \frac{P_T A_T A_R}{\lambda^4 d^4} \cdot 16 \cdot c^2 b^2 \psi^2 |R_o|^2 \qquad (4.19)$$

Normally,

$$P_D = \frac{P_T G_T}{4\pi d^2/4} \cdot \sigma_s \cdot \frac{1}{4\pi d^2/4} \cdot A_R$$

since $G_T = \frac{4\pi A_T}{\lambda^2}$,

$$P_D = \frac{P_T A_T A_R \cdot 16 \cdot \sigma_s}{4\pi \lambda^2 d^4} \qquad (4.20)$$

Comparing 4.20 and 4.19 , we find the bistatic radar reflection area, σ_s, as

$$\sigma_s = \frac{4\pi}{\lambda^2} \cdot c^2 b^2 \psi^2 |R_o|^2 \qquad (4.21)$$

We know from 4.9 that

$$P_{FS} = \frac{P_T G_T G_R}{(4\pi)^2 d^2}^2 \quad , G_T = \frac{4\pi A_T}{\lambda^2} \, , \; G_R = \frac{4\pi A_R}{\lambda^2}$$

substituting the above in 4.20 , we get

$$P_D = P_{FS} \cdot \frac{4\sigma_s}{\pi d^2} \qquad (4.22)$$

4.22 now gives the power received by reflection from one surface lying somewhere in midpath.

$$\text{Total } P_D = P_{FS} \cdot \frac{4}{\pi d^2} \int_V N \; \sigma_s \; dV \qquad (4.23)$$

where N is the number of reflecting facets per m^3.

4.2.6 Conversion of Volume Integral into Height Integral

The integral in expression(4.23) now being easily solvable we convert this into a height integral, following Gordon[7], using his concept of scattering angle dependance on scattered power received.

Since the scattered power is proportional to an inverse power of θ, the important scattering will occur in a volume in which the angle is at or near its minimum value. This minimum occurs at the intersection of the horizon planes of the transmitter and receiver in the plane of propagation. At this point the value of θ is d/a, as indicated in Fig. 4.2. The horizon planes will form the lower boundary of the scattering volume. Now the length, l, of scattering volume will be given by

$$\frac{h}{l/2} = \tan \frac{d}{2a_e} \qquad (4.24)$$

For small θ, $l = 2h(2a_e/d)$ (4.24)

Now refering to Fig. 4.3, define a width w along the intersection of the horizon planes (i.e. perpendicular to the plane of propagation) by the condition that the scattering cross section at the edge P_1 is one-half that at the centre point P_o. Scattering cross-section, σ, is defined as the power measure per unit solid angle, per unit incident power intensity and per unit volume, and is given by Gordon[7] as

$$\overline{\nabla}(\theta) \propto \frac{1}{\theta^4} \quad \text{for small } \theta \,. \tag{4.25}$$

Now, the important volume will be taken as a vertical slab of constant width w. The condition on scattering section reduces with (4.25) to

$$\theta_o^4 = \frac{1}{2}\theta_1^4 \tag{4.26}$$

In Fig. 4.3, plane TABR is the vertical plane through the transmitter and receiver, whereas TA'B'R is the plane indicating the width w, as defined above. The angles θ_o and θ_1 are contained in these two planes respectively. Now the half-width w/2 is

$$\left(\frac{w}{2}\right)^2 = \left(\frac{\theta_1}{2} \cdot \frac{d}{2}\right)^2 - \left(\frac{\theta_o}{2} \cdot \frac{d}{2}\right)^2$$

With (4.26)

$$w = \frac{1}{3}\,\frac{d^2}{a} \tag{4.27}$$

The volume integration now reduces to an integration of height h, in which an element of volume is the product of width w, a length l and an elemental height dh. No (4.23) reduces to

$$\text{Total } P_D = P_{FS} \cdot \frac{4}{\pi d^2} \int_h N \cdot \overline{\nabla_s} \cdot \frac{1}{3} \cdot \frac{d^2}{a} \cdot \frac{2h \cdot 2a}{d}\, dh$$

$$\text{or} \quad P_D = P_{FS} \cdot \frac{16}{\pi d \cdot 3} \int_h N \cdot \overline{\nabla_s} \cdot h \cdot dh \tag{4.28}$$

4.3 Prediction Technique

(a) The terrain profile in the present prediction system is prepared in the same manner as in NBS 101, with the difference that effective earth radius is calculated from the median value of refractivity gradient appropriate for the path. This has to be determined for the time block, and months or season for which prediction is desired.

(b) Path parameters like the horizon distances, effective antenna heights etc. are also determined following NBS 101.

(c) The actual calculation for signal strength is made following Eklund and Wickert's model, by finding C_n^2 from an empirical relationship with ΔN_1

$$\text{Log}_{10} C_n^2 = -17 + 0.023 (-47 - \Delta N_1)$$

Here sign of ΔN_1 is to be taken into account.

(d) While calculating P_D, due to reflection, this model does not allow for the effect of super-refraction due to high gradients of refractivity. Super-refraction influences the reflected signal by bringing down the height of common volume, thus reducing the angle of reflection and increasing the available number of reflecting glints. Both these factors increase the field strength. In this method, the

effect of super-refraction is taken into account by means of the term in bracket in the following expression, which is a modification of (4.23).

$$\frac{P_D}{\Gamma_{FS}} = \frac{4}{\pi d^2} \left[\frac{\frac{dM}{dh}}{\frac{dM_m}{dh}} \right]^{-14/3} \int_V N \cdot \nabla \cdot \, dV \qquad (4.29)$$

Where M_m is the long term median value of the modulus.

(e) For gradient values representing ducting conditions, the field strength is calculated by mode theory of propagation in a duct.

(f) For gradients between -130 N units/Km and ducting situation, the field strength is obtained by interpolation.

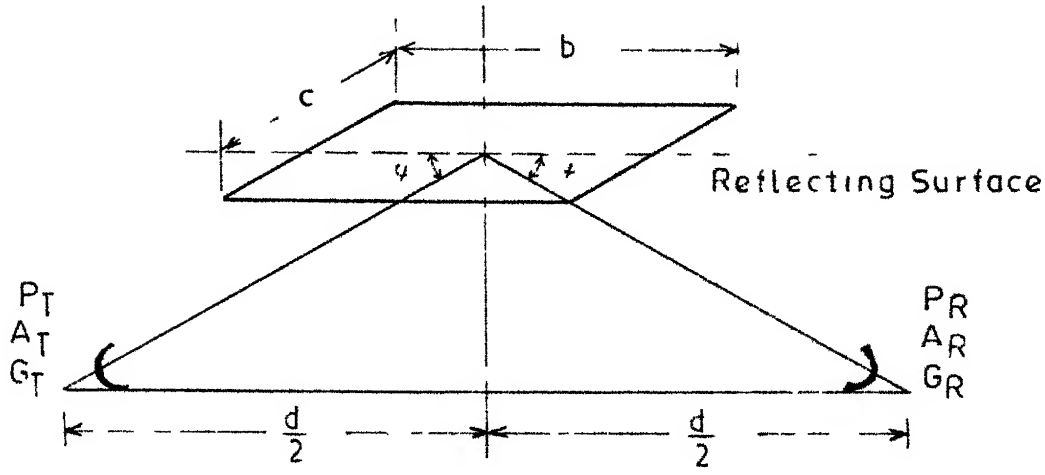

FIG 4.1 REFLECTION FROM A LAYER

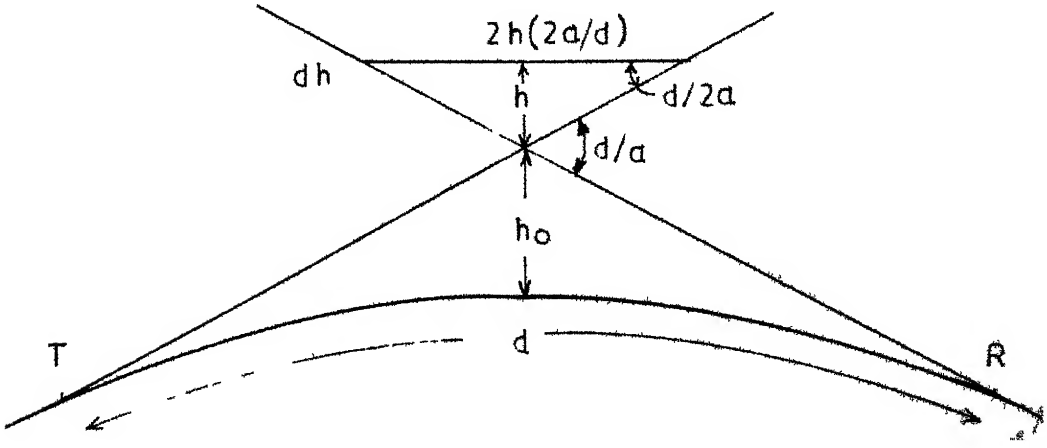

FIG. 4.2 GEOMETRY OF COMMON VOLUME

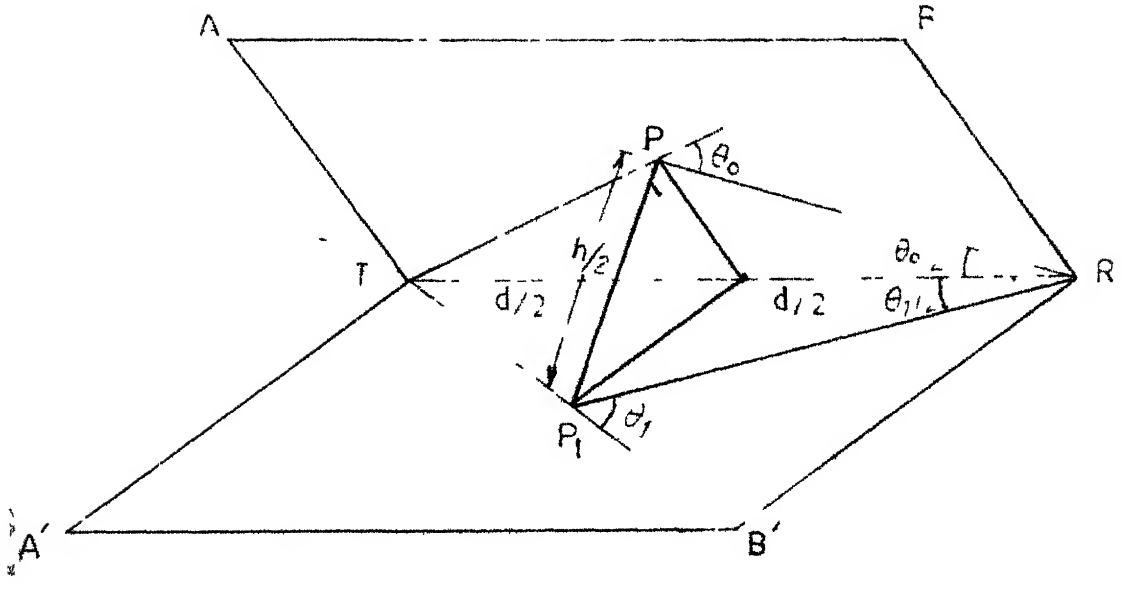

FIG 4 3 WIDTH OF THE COMMON VOLUME

CHAPTER 5

OTHER METHODS

5.1 CCIR (French Administration Method)

CCIR[1] report 238-2 provides a method for calculation of transmission loss for cases where radiometeorological parameters are available. Studies conducted by French Administration have shown that attenuation between isotropic antenna could be represented by a formula, which appeared to be valid for all climates, given as

$$L_b = 20 \log (fd) + 10 \log(fD_s) + K_1(D_s) - K_2(D_s\,\theta) - T$$

where L_b is the attenuation, in dBs, between isotropic antenna,

d is the distance between antennas in Kms,

f is the frequency in MHz.,

D_s is the distance, in Kms, between radio horizons for median atmospheric conditions,

θ is the scatter angle in radians,

$K_1(D_s)$ is defined by Fig. 5.1,

$K_2(D_s\theta)$ is defined by Fig. 5.2 and

T is a parameter determined from meteorological soundings, as described in report 233-3 and succeeding paragraphs.

In this method an attempt has been made to improve the correlation between the variations of signal strength observed in the field and the refractivity gradient, ΔN, by considering atmospheric conditions in the neighbourhood of common volume.

A parameter, T, as defined below, was demonstrated to be representative of monthly mean path attenuation for very different distances and climates.

$$T = a\,G_e + b\,G_c \quad \text{dBs}$$

where a & b have been determined experimentally as

$$a = \frac{-3}{8} \quad \text{and} \quad b = \frac{-5}{4}$$

G_e is the equivalent gradient between the ground and the common volume (which can often be replaced by ΔN at 1 Km above the ground), G_c is $\angle^{\text{the}}$ difference between the value of N at a point situated 1 Km above the base of the common volume, and the value at the base of the common volume. If G_e is approximated to be ΔN_1, then data for determining its value is currently available from Radio Refractivity Atlas. G_c can be determined using this semi-emperical formula

$$G_c = \frac{1}{3}(200 - N_s - \frac{2}{3}G_e) \text{ for } 1 \text{ Km} < D_s\theta < 2.7 \text{ Km}$$

$$\frac{3}{7}(200 - N_s - \frac{2}{3}G_e) \text{ for } D_s \geqslant 2.7 \text{ Km}.$$

5.2 Collins Method

This is a method contained in an instructional manual for the U.S. Army[23], and was prepared by the Collins Radio Company. The method is entirely graphical and is suitable

for quick prediction of path loss for field siting of mobile troposcatter communication equipment.

(a) The path length is determined using same formula as given in Chapter 2 (Section 2.2). The distance in statute miles is given by

Z(in degrees) x 69.093 = d (statute miles)

where Z is the spherical triangle distance between the two antennae.

(b) Horizon angles are determined by using figures 5.3 and 5.4 and topographical maps. Starting at transmitter, find the highest elevation points along the line towards the receiver. The difference between the elevation at one of these points, and the transmitter site is found. Depending on the distance between the transmitter antenna, and this elevation point, Fig. 5.3 or Fig. 5.4 is used to determine the horizon angle. This is repeated for all high elevation points, till the maximum horizon angle is found.

(c) Repeating (b) above for receiver, it's maximum horizon point is also determined. Both these horizon angles are added to find the sum of horizon angles for the circuit.

(d) A path profile can also be drawn on a 4/3 earth profile paper, and distance and elevation values can be determined from this straight away.

(e) Basic propagation loss is determined from Fig. 5.6 (which gives the loss for 1000 MHz.). Correction for frequency is obtained from Fig. 5.8 which is simply a plot of 30 log f, with the origin suitably placed. This combined loss gives the basic propagation loss for the circuit.

(f) Loss due to elevated horizon angles is found using Fig.-5.5 a set of curves for varying distances, to allow for loss variations when the horizon angles are non-zero. Majority of curves are for positive elevation angles, and there is a very small range of negative elevation angles.

(g) Nomograms have also been made for determining the following.

i) Antenna gain and beamwidth from frequency and reflector diameter (Fig. 5.7).

ii) Aperture-to-medium coupling loss from distance and antenna beamwidth (Fig. 5.9).

This method uses the 4/3 standard earth atmosphere and no knowledge of local radiometeorological parameters (N_s or ΔN_1) is necessary. Hence no correction for difference in various climates are possible.

5.3 Parl's Method

In a recent paper, Parl[16] has evolved a general formula for basic tropospheric path loss, in terms of

spectrum slope, refractive index variance, and scale of turbulence.The refractive index fluctuations have been characterised by its covariance function, defined as

$$\phi_n(\vec{r}_1, \vec{r}_2) = E\left[n_1 (\vec{r}_1) \, n_2 (\vec{r}_2) \right]$$

where $n_1(\vec{r}) = n(\vec{r}) - E[n(\vec{r})]$, for $n(\vec{r})$ being the refractive index at a point with coordinates $\vec{r}$. Parl has considered the volume of troposphere to be homogeneous and isotropic. For homdgeneous medium, the covariance is only a function of $\vec{r} = \vec{r}_1 - \vec{r}_2$. Following Tatarski[20], we get the wavenumber spectrum as

$$\Phi_n(k) = \frac{1}{(2\pi)^3} \iiint \phi_n(\vec{r}) \exp(i \vec{k} \cdot \vec{r}) \, d^3 \vec{r} \qquad (5.1)$$

For an isotropic atmosphere, the wave-number spectrum is only a function of the magnitude k of the wavenumber vector $\vec{k}$.

Again following Tatarski[20], Parl gives the effective cross section of scattering a_s, of a small volume dV as

$$a_s = 8\pi^2 K^4 \Phi_n\left[2K \sin \theta/2 \right] dV \qquad (5.2)$$

where θ is the scattering angle. Tatarski's equation (1.27) gives 3-dimensional wavenumber spectrum for an isotropic field as

$$\Phi(k) = \frac{1}{2\pi k} \frac{dV(k)}{dk} \qquad (5.3)$$

where V(k) is the one-dimensional spectrum. Equation (1.29) shows correlation function, $B_f(x)$, to be a fourier integral of V(k), that is

$$V(k) = \frac{1}{2\pi} \int_{-\infty}^{\infty} e^{-jkx} \; B_f(x)\, dx \qquad (5.4)$$

A correlation function, of the form mentioned below, was proposed by Von Kármán as an approximation to the correlation functions arising in the theory of turbulence

$$B_f(r) = \frac{a^2}{2^{\nu-1}\Gamma(\nu)} \left(\frac{r}{r_o}\right) K_\nu \left(\frac{r}{r_o}\right), \quad \nu>0 \qquad (5.5)$$

Where a^2 is the variance of the random field, r_o is the correlation distance of the turbulence, $K_\nu(x)$ is the Bessels function of 2nd kind of an imaginary argument.

As per Tatarski[20] equation 1.35, using equations (5.5), (5.4) and (5.3) above, and substituting $\nu = \frac{m-3}{2}$, we get the wavenumber spectrum as

$$\Phi_n(k) = \frac{2^2 \left\lceil \frac{m}{2}}{\pi^{3/2} \left\lceil \frac{m-3}{2}} \; r_o^{3/2} \left(1+k^2 r_o^2\right)^{\frac{-m}{2}} \quad m>3 \qquad (5.6)$$

If $\Phi_n(k)$ is plotted on a doubly logarithmic scale, the slope falls off as 'm', and hence 'm' is called the spectrum slope. The wavelength $\lambda = 2\pi/k$ is assumed to be in the inertial subrange, that is,

$$l_o << \lambda << L_o$$

Where l_o and L_o are the inner and outer scales of turbulence respectively. r_o in (5.6) can usually be identified with L_o. As already discussed in Chapter 4, the power received from a small scatterer at a point r, and with the cross section a_s, is

$$P_R(r) = P_T \cdot \frac{G_T(\vec{r})}{4\pi R_T^2(\vec{r})} \cdot \frac{a_s(\vec{r})}{4\pi R_R^2(\vec{r})} \cdot \frac{\lambda^2 G_R(\vec{r})}{4\pi} \qquad (5.7)$$

where $P_T(P_R)$ = Transmitted (Received) power

$G_T(\vec{r})(G_R(\vec{r}))$ = Gain of Transmitter(Receiver) antenna towards the scattering point $\vec{r}$.

$R_T(\vec{r})(R_R(\vec{r}))$ = Distance from transmitter (receiver) to the scattering point $\vec{r}$.

Using (5.6) in (5.1), and assuming $Kr_o >> 1$, we get the received power as

$$P_R = P_T \cdot C \iiint \frac{G_T(\vec{r}) G_R(\vec{r})}{R_T^2(\vec{r}) R_R^2(\vec{r})} \left(2 \sin \frac{\theta(\vec{r})}{2}\right)^{-m} d^3\vec{r} \qquad (5.8)$$

where $C = \nabla_n^2 \, r_o^{3-m} \, k^{2-m} \Gamma(\frac{m}{2}) / [2\sqrt{\pi} \, (\frac{m-3}{2})]$

and range of integration is the common volume V. It has been assumed that ∇_n^2 and r_o do not vary appreciably throughout the common volume. Substituting the value of m = 11/3 gives us the Kolmogorov - Obukhov theory of turbulence. Setting m=5, gives us the expression used by NBS 101[17] model. This general expression can also be used for other values of m,

if found necessary. For any prediction of P_R, we will need to specify m, r_o and $\overline{\nu_n^2}$.

Carl has further derived an expression for approximate path loss for omnidirectional antennas (with minimum scatter angle, θ_s, small), which can be relaxed to fit cases of wide beam antennas (beam wide enough to encompass the main scattering volume). For omnidirectional antennas, basic path loss is

$$\frac{P_R}{P_T} = \overline{\nu_n^2} \; r_o^{3-m} \; k^{2-m} \; \frac{(m-3)}{4(m-1)(m-2)} \frac{(\theta_s^{2-m})}{d} \quad , m > 3 \tag{5.9}$$

For wide beam antennas, (5.9) must take into account the antenna gains also.

In a comparison between m=5 (NBS 101 model) and m=11/3 (Turbulent scatter model) for the above path loss, we find the frequency dependence for m=5 to be cubic (f^{-3}), while for m=11/3, it works out much weaker ($f^{-5/3}$). Hence turbulent scatter provides dominant transmission at higher frequencies. The following conclusions can be drawn from above

(a) In general, it is not possible to use a single model (fixed m) to compare performances at different frequencies and distances.

(b) If only one model were to be used, it is better to base the link design on turbulent scatter (m=11/3) model. This model is more accurate at high frequencies and is useful at lower frequencies to estimate the performance when atmospheric layering is absent.

For narrow antenna beams, Parl has introduced Aperture-to-medium coupling loss concept, taking various cases of antenna beamwidth. This aspect could not be included in this thesis due to shortage of time. Also no analytical work could be done due to same reasons.

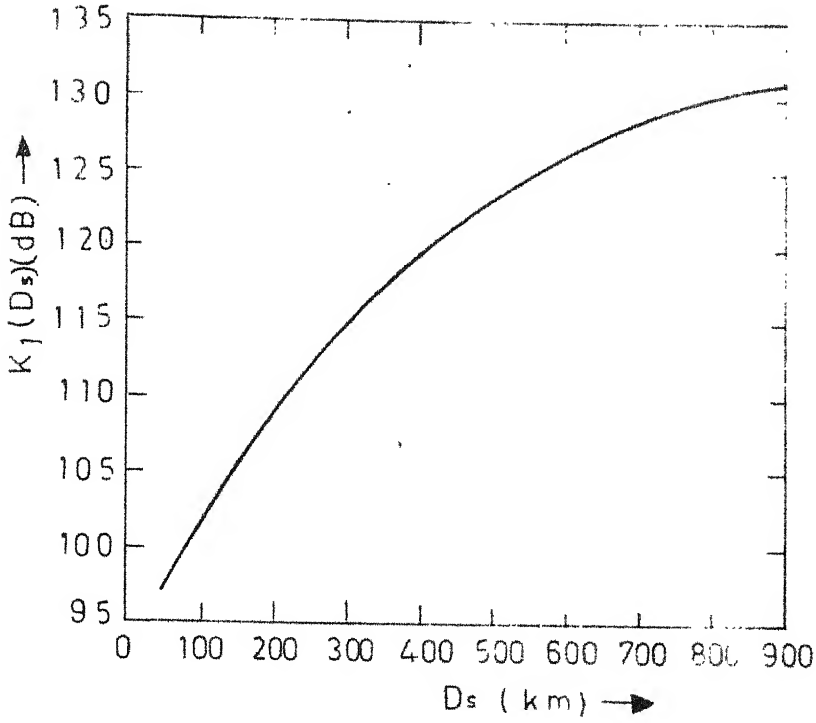

FIG.5.1 FUNCTION $K_1(D_s)$

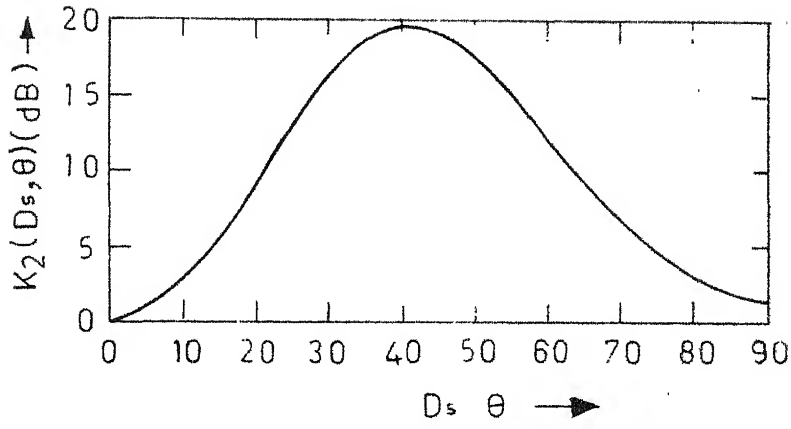

FIG.5.2 FUNCTION $K_2(D_s\theta)$

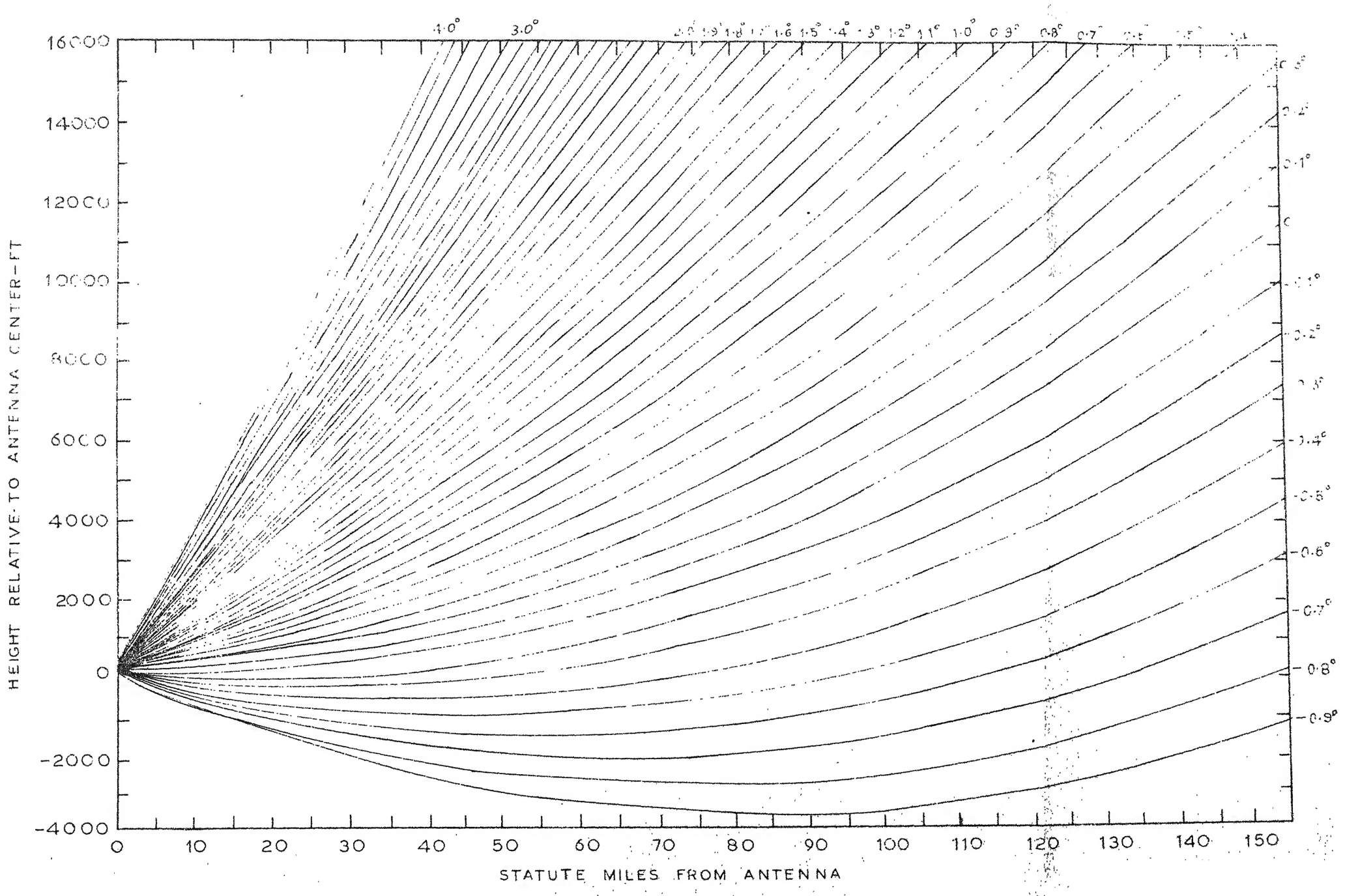

FIG. 5.3 HORIZON ANGLE DETERMINATION CURVES FOR LONG DISTANCES

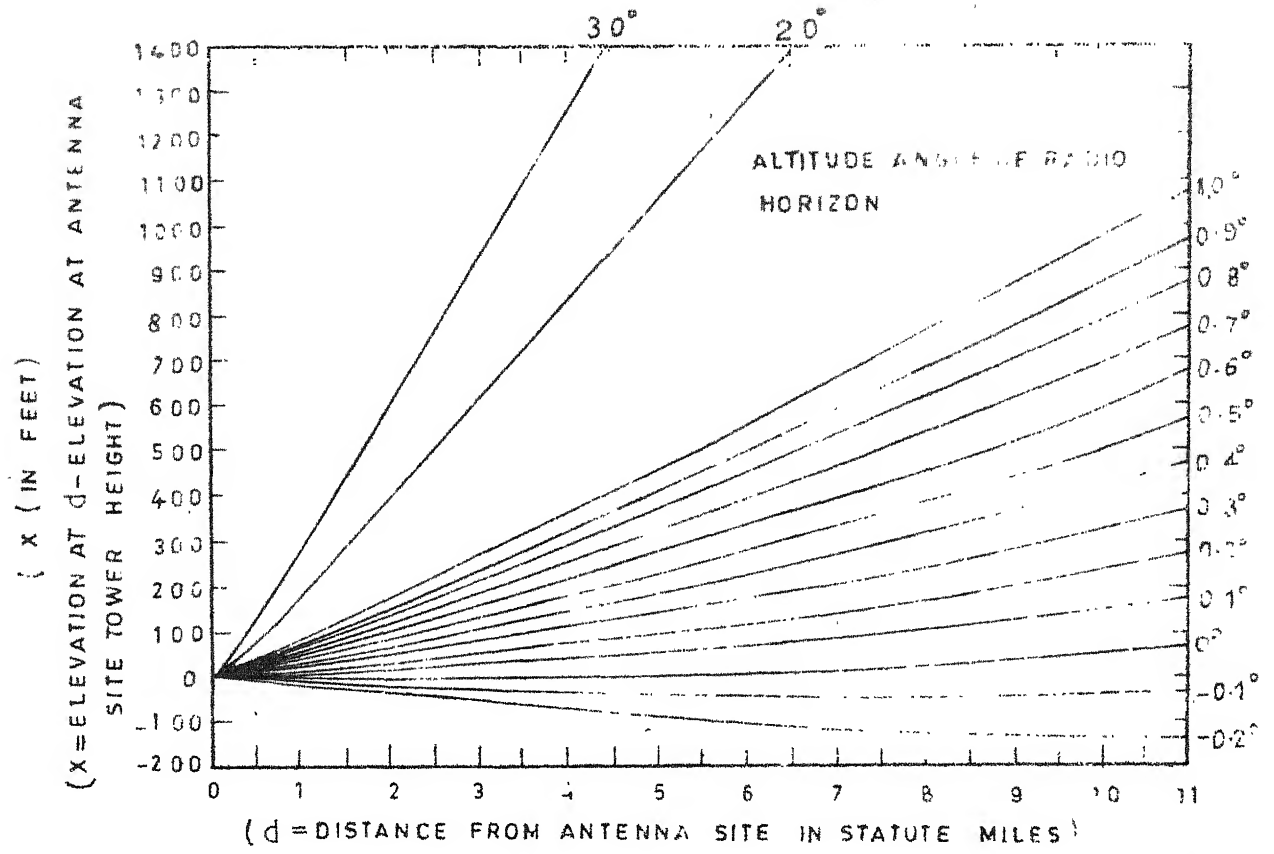

FIG.5.4 HORIZON ANGLE DETERMINATION CURVES FOR SHORT DISTANCES

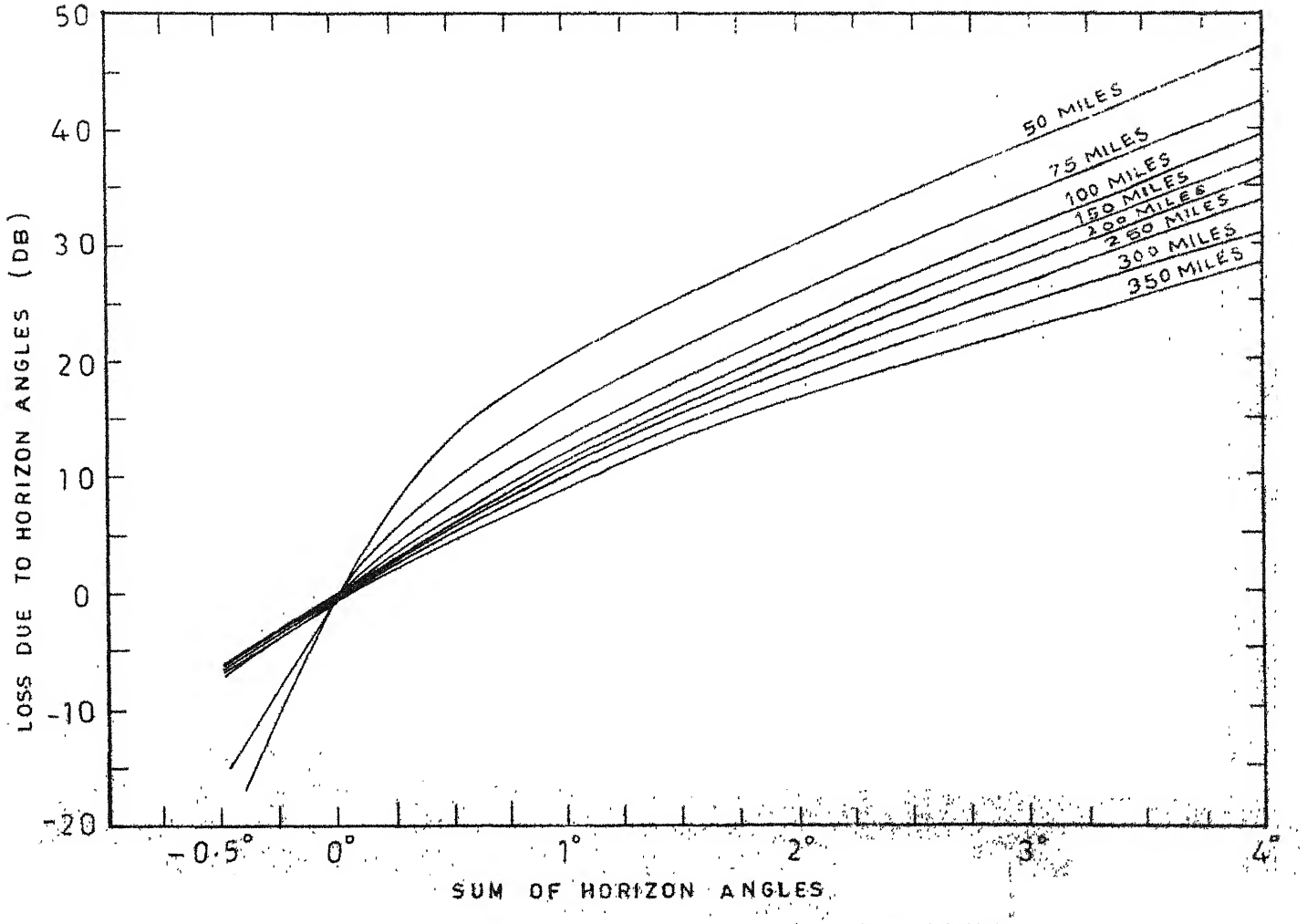

FIG.5.5 LOSS DUE TO ELEVATED HORIZON ANGLES

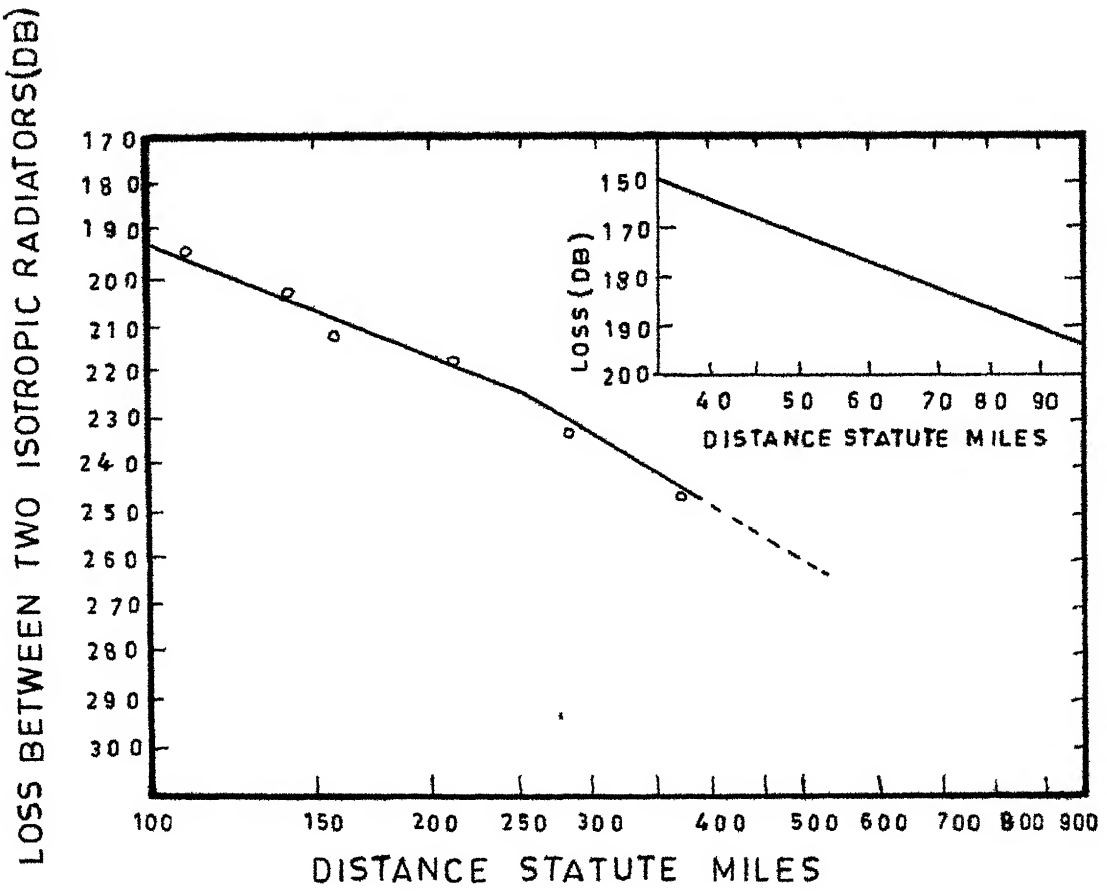

FIG 5 6 BASIC PROPAGATION LOSS CURVE FOR 1000 MEGACYCLES

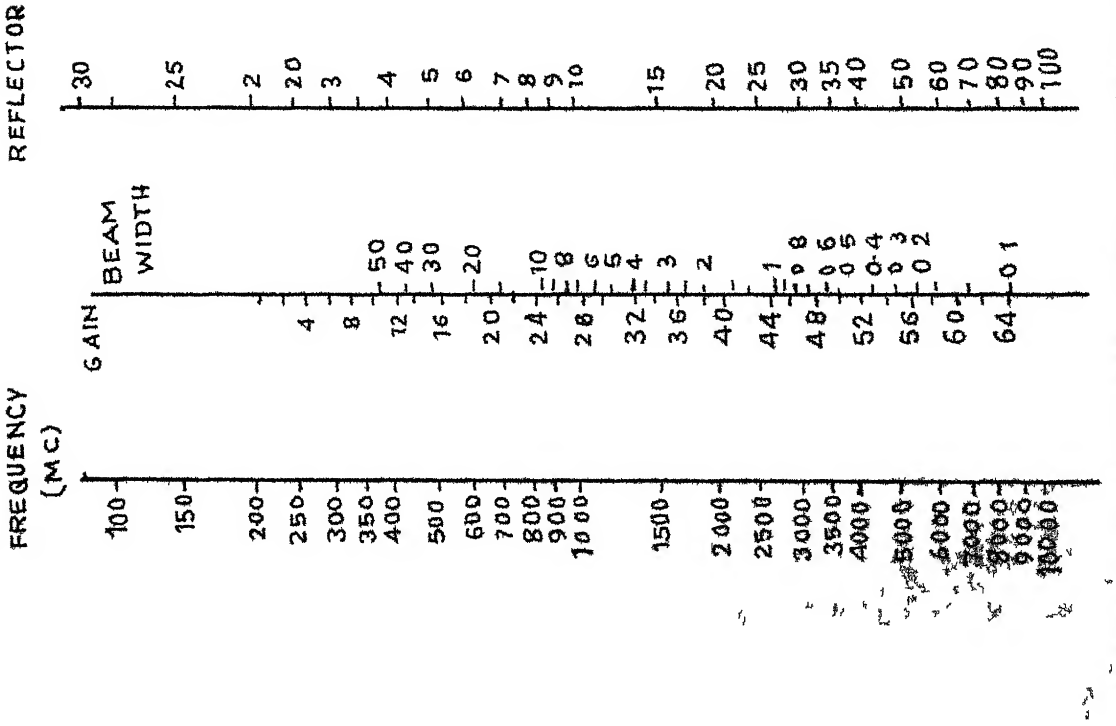

FIG.5.7 NOMOGRAM FOR DETERMINING ANTENNA GAIN AND BEAM WIDTH

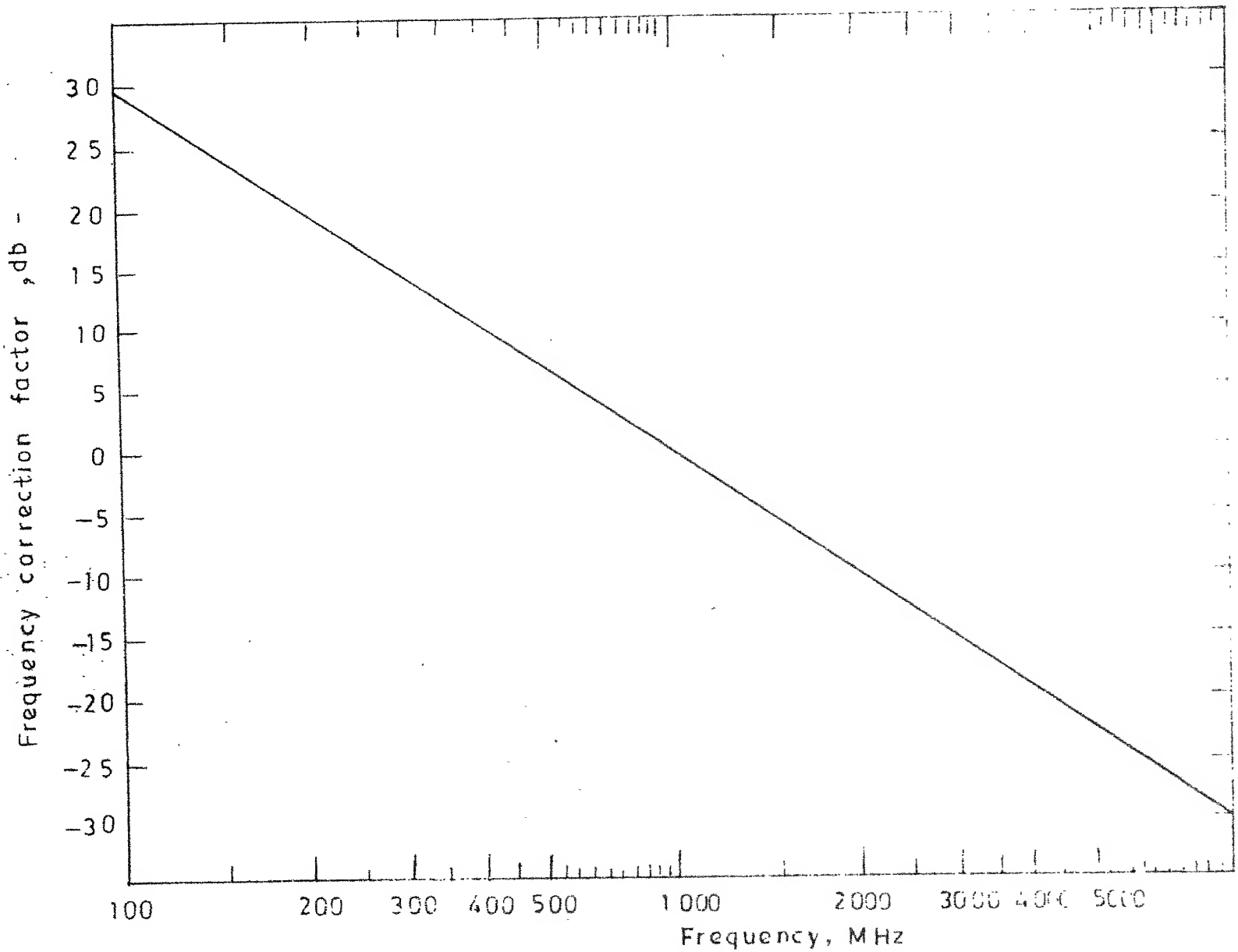

FIG. 5.8 FREQUENCY CORRECTION CURVE FOR BASIC PROPAGATION LOSS.

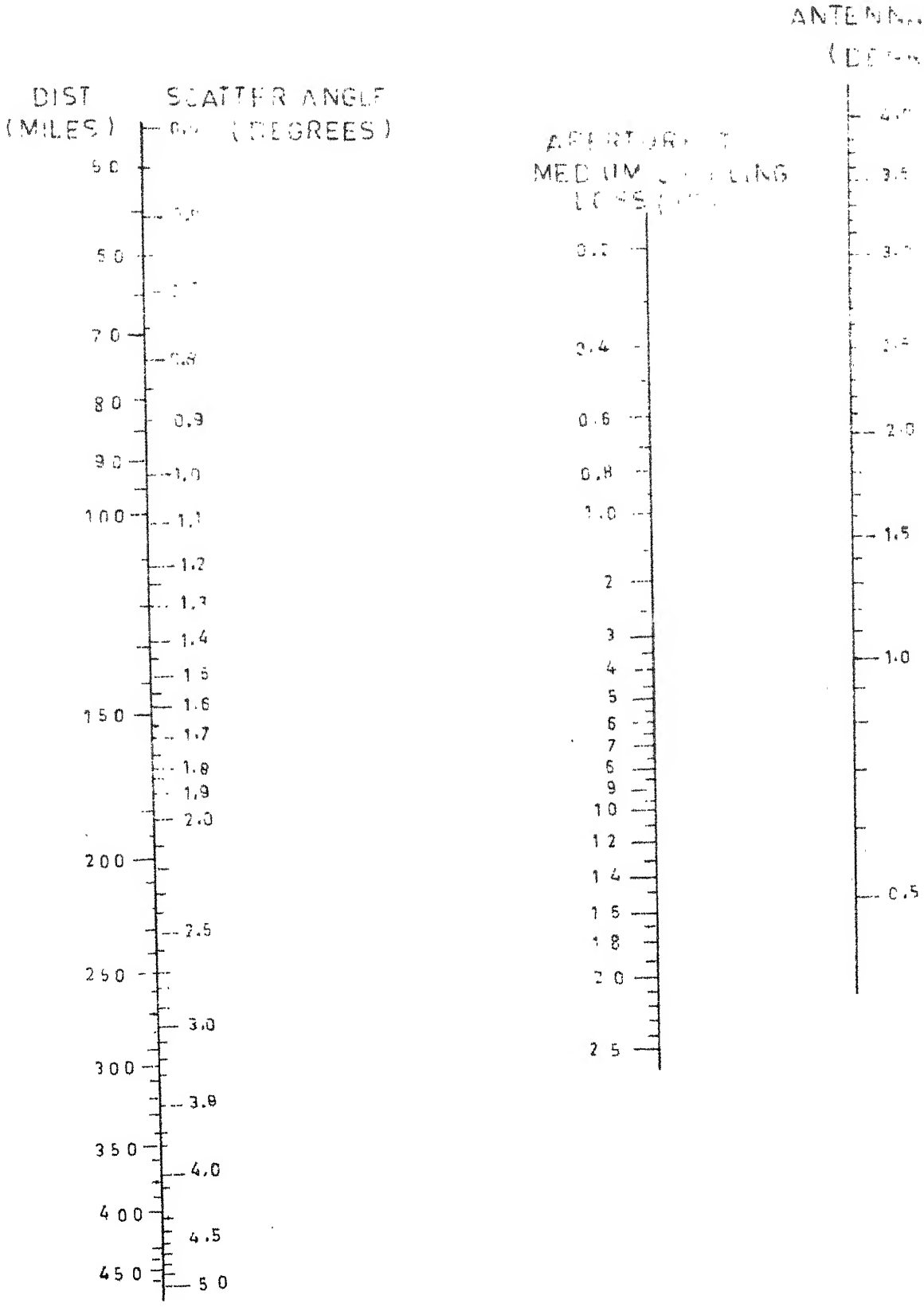

FIG.5.9 NOMOGRAM FOR DETERMINING APERTURE TO MEDIUM COUPLING LOSS.

CHAPTER 6

INTERCOMPARISON OF VARIOUS METHODS

6.1 Path Loss Comparison

(a) A comparison of median path loss as obtained from different methods, along with all other related parameters, for Kanpur-Nainital link is tabulated in Table 6.1.

(b) A comparison between observed and predicted path losses (by NBS 101 and NPL methods only, being the prominent methods) on monthly basis for fixed hours has been done and plotted as follows

i) Observed 0600 hrs, NBS 101 0600 hrs and NPL 0530 hrs in Fig. 6.1.

ii) Observed 1800 hrs, NBS 101 1800 hrs and NPL 1730 hrs in Fig. 6.1.

iii) Observed 1800 hrs, NBS 101 1730 hrs. in Fig. 6.2.

(c) A cumulative distribution of predicted path loss by NBS 101, NPL method and the observed path loss has been plotted in Fig. 6.3.

6.2 Sources of Data

6.2.1 Effective Earth Radius, a_e. In Section 3.2 it was mentioned that the initial refractivity gradient, ΔN_1, should be read from Radio Refractivity Atlas[12] and used for

calculation of a_e. Majumdar's[10] correlation of $\overline{\Delta N_1}$ with $\bar{N}_s$ for the three inland radiosonde stations, Allahabad, Delhi and Nagpur has been given as 0.66, 0.36, and 0.76 respectively. Based on this he has evolved the empirical relationship, for inland regions, as given in Section 3.2. The contours of ΔN_1 in Radio Refractivity Atlas are based on data collected from 16 radiosonde stations over a period of 4 years (1968-71). ΔN_1 was calculated fron N_s values for Kanpur-Nainital region and compared with the corresponding ΔN_1 values. A vast difference was found between the two. The annual mean N_s for Kanpur-Nainital region was worked out to 315.6 N-units. The gradient calculated from this, using Majumdar's $\angle$ model, works out to 36.06 N-units/Km, whereas the annual mean $\overline{\Delta N_1}$, read from Atlas, works out to 66.25 N-units/Km. Also, Majumdar[10] has given (in his Fig. 6.1(b)) representative mean values of refractivity gradient for different regions of India. The value for Northern and Central Plains varied between -50 to -70 N-units/Km. Based on this, and on the fact that correlation of $\overline{\Delta N_1}$ with $\bar{N}_s$ for atleast one inland radiosonde station (Delhi) was found to be poor, we reject the empirical model for determining ΔN_1 from N_s. Hence the effective earth radius has been calculated, in this thesis, by using refractivity gradient, read from the Atlas, appropriate to the path and time of the year.

6.2.2 NBS 101 Method

(a) The mean value of N_s for median path loss has been calculated by using the mean value of surface refractivity reduced to mean sea level, N_o, read from Majumdar[11], in the following expression

$N_s = N_o \exp(-0.1057\, h_s)$ where h_s is the elevation of the surface above mean sea level in kilometers.

(b) The values of N_s for 6.1(b) (i) and (ii) above have been taken from Pande[15], and are the values measured at Delhi. The values of N_s for 6.1(b) (iii) above have been taken from Girdhar[27] and are those measured at Lucknow.

(c) For plotting 6.1(c) above, the method mentioned in NBS 101 has been used. Majumdar[11], after Venkiteswaran[24], has classified the region of Kanpur-Nainital line, as per classification of NBS 101, as 'Continental Temperate' from November to May, and 'Equatorial' from June to October. Using the data given in NBS 101(vol. II)[17] for these two climatic regions, the weighted mean values of $V(0.5, d_e)$ was found. Also the functions $Y(q, d_e, 100\ MHz)$ for $q = 0.1$ and $q = 0.9$ were similarly determined from data in NBS 101 vol. II. Now,

$Y(q,f) = Y(q, d_e, 100\ MHz)\ g(q,f)$ for $q=0.1$ and $q = 0.9$

where g(q,f) is the 'frequency factor'. For frequencies above 1.6 GHz it can be taken as 1.05 (from Computer Code[9]). To estimate the other percentile levels, the following empirical relationships from NBS 101 (for 'Continental Temperate' Climate) were used

$$Y(0.0001) = 3.33\ Y(0.1) \qquad Y(0.9999) = 2.90\ Y(0.9)$$

$$Y(0.001) = 2.73\ Y(0.1) \qquad Y(0.999) = 2.41\ Y(0.9)$$

$$Y(0.01) = 2.0\ Y(0.1) \qquad Y(0.99) = 1.82\ Y(0.9)$$

6.2.3 NPL Method

(a) The mean value of initial refractivity gradient, ΔN_1, has been obtained from initial refractivity gradient contours, for different months (0000 hrs and 1200 hrs GMT), read from Radio Refractivity Atlas[12].

(b) Data of ΔN_1 for plots mentioned in 6.1(b) above has also been read from Radio Refractivity Atlas[12].

(c) Data of ΔN_1 for cumulative distribution in 6.1(c) has been read from the cumulative distribution curves in the Atlas, for 'Northern Plains', and the mean obtained.

(d) Volume integral in this method has been converted to a height integral by the method mentioned in Chapter 4. Since no data was available regarding the number of reflecting facets per (metre)^3, the values mentioned in Eklund and

(i) 0600 hrs NPL method tends to correlate to observed values for period April-July, whereas NBS 101 seems to vary in accordance with observed in the period July-November. No other similarity of any nature is observed.

(ii) 1800 hrs. NPL method appears to correlate for the period February-May, but variations in predictions by NBS 101 (Delhi Data - Fig. 6.1), though some what subdued, tend to agree with variations of observed path loss for the period January-August. For Lucknow data (Fig. 6.2), the NBS 101 does not vary very greatly from observed values (at most, upto 10 dBs), and appears to be in perfect agreement for the months of August and September.

(c) The structure constant, C_n^2 , (used in NPL method) for the median yearly ΔN_1, relative to Kanpur-Nainital region works out to 2.77×10^{-17} $(cm)^{-2/3}$ and does not compare favourably with the values quoted by Majumdar[10] (5×10^{-15} to $10^{-13}(cm)^{-2/3}$ for Delhi region), but agrees well with the figures quoted by Eklund and Wickerts[4] (2.5×10^{-16} to 6.3×10^{-19}).

(d) At this frequency (2100 MHz), the reflection mode of propagation was found to be dominating. Our value of 10 $\log_{10}$ (P_R/P_{FS})(-62.8 dB) was found to be higher than that obtained from relevant curves (approx. -75 dB) given by Eklund and Wickerts[4].

Table 6.1

Sl. No.	Parameter	NBS 101 Method	NPL Method	CCIR Method	Collin's Method	Units
1.	Surface Refractivity (N_s)	315.6	-	315.6	-	N units
2.	Initial Refractivity Gradient($\triangle N_1$)	-66.25	-66.25	-66.25	-40	N-units
3.	Effective Earth Radius (a_e)	11021.0	11021.0	11021.0	8493.33	Kms
4.	Scatter Angle (θ)	0.029	0.029	0.029	-	radians
5.	Function(F(θd))	167.32	-	-	-	dBs
6.	Function F_o	-1.089	-	-	-	dBs
7.	Function H_o	0.0	-	-	-	dBs
8.	Spectral Intensity of refractive index fluctuations. (C_n^2)	-	0.2772×10^{-16}	-	-	$cm^{-2/3}$
9.	Power reflection coefficient($\|R_o\|^2$)	-	0.383×10^{-7}	-	-	
10.	Bistatic Radar Area, $\sqrt{\sigma_s}$	-	0.297	-	-	m^2
11.	P_S/P_{FS}	-	$.823 \times 10^{-9}$	-	-	

contd...

Sl. No.	Parameter	NBS 101 Method	NPL Method	CCIR Method	Collin's Method	Units
12.	P_D/P_{FS}	-	0.117×10^{-6}	-	-	
13.	P_R/P_{FS}	-	0.118×10^{-6}	-	-	
14.	Meteorological loss parameter (T)	-	-	62.57	-	dBs
15.	Function $K_1(D_s)$	-	-	116.25	-	dBs
16.	Function $K_2(D_s)$	-	-	2.5	-	dBs
17.	Basic Path Loss (1000 MHz.)	-	-	-	219 (for 203 statute miles)	dBs
18.	Frequency Correction	-	-	-	-10.5	dBs
19.	Loss due to elevated horizon angles	-	-	-	0.0	dBs
20.	d_e	196.59	-	-	-	Kms
21.	$V(0.5, d_e)$	5.48	-	-	-	Kms
22.	Median Basic Path Loss	216.00	218.4	225.68	208.5	dBs

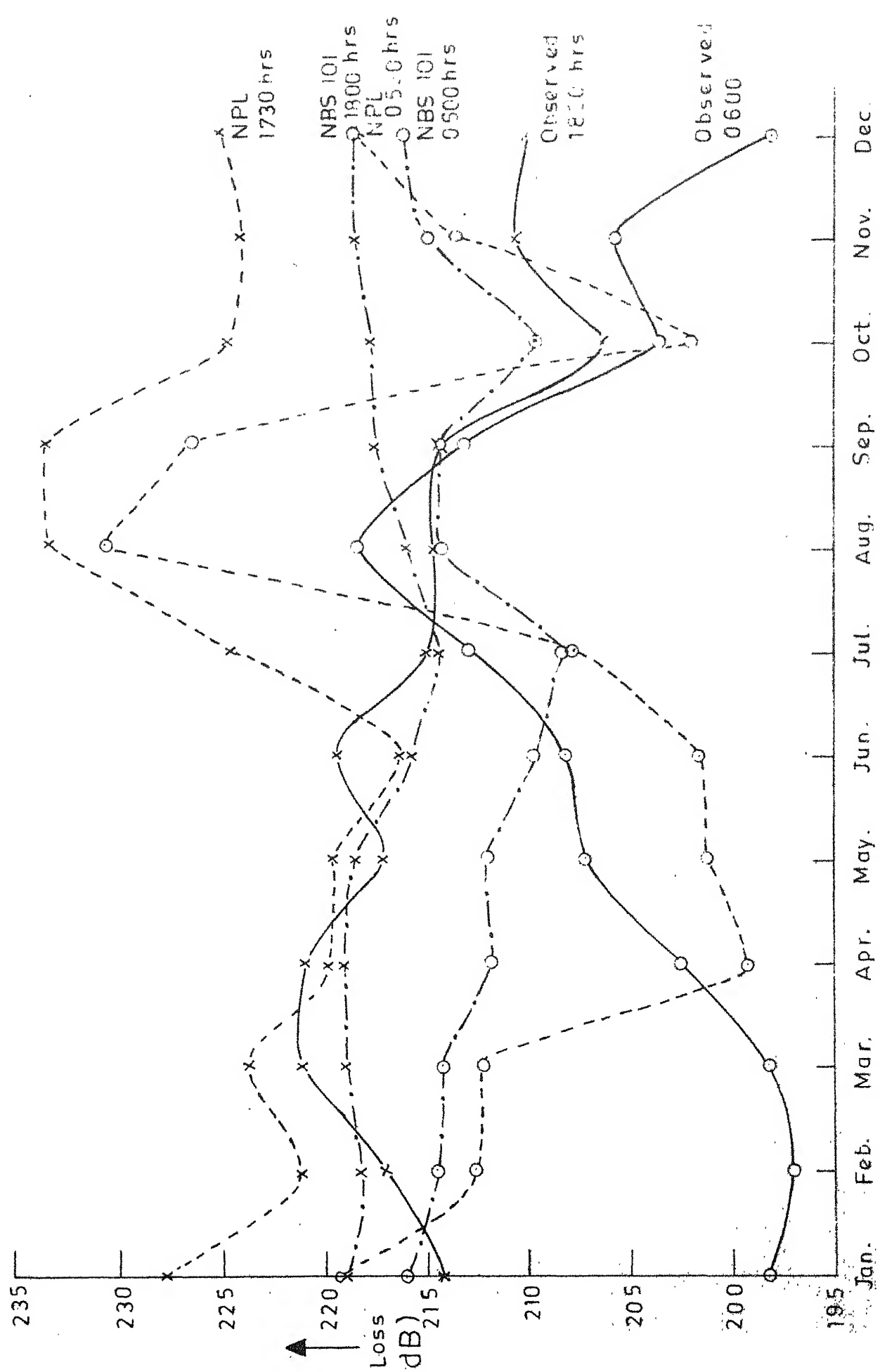

FIG. 6.1 YEARLY DISTRIBUTION OF PATH LOSS AT 0600 hrs AND 1800 hrs, KANPUR – NAINITAL LINK.

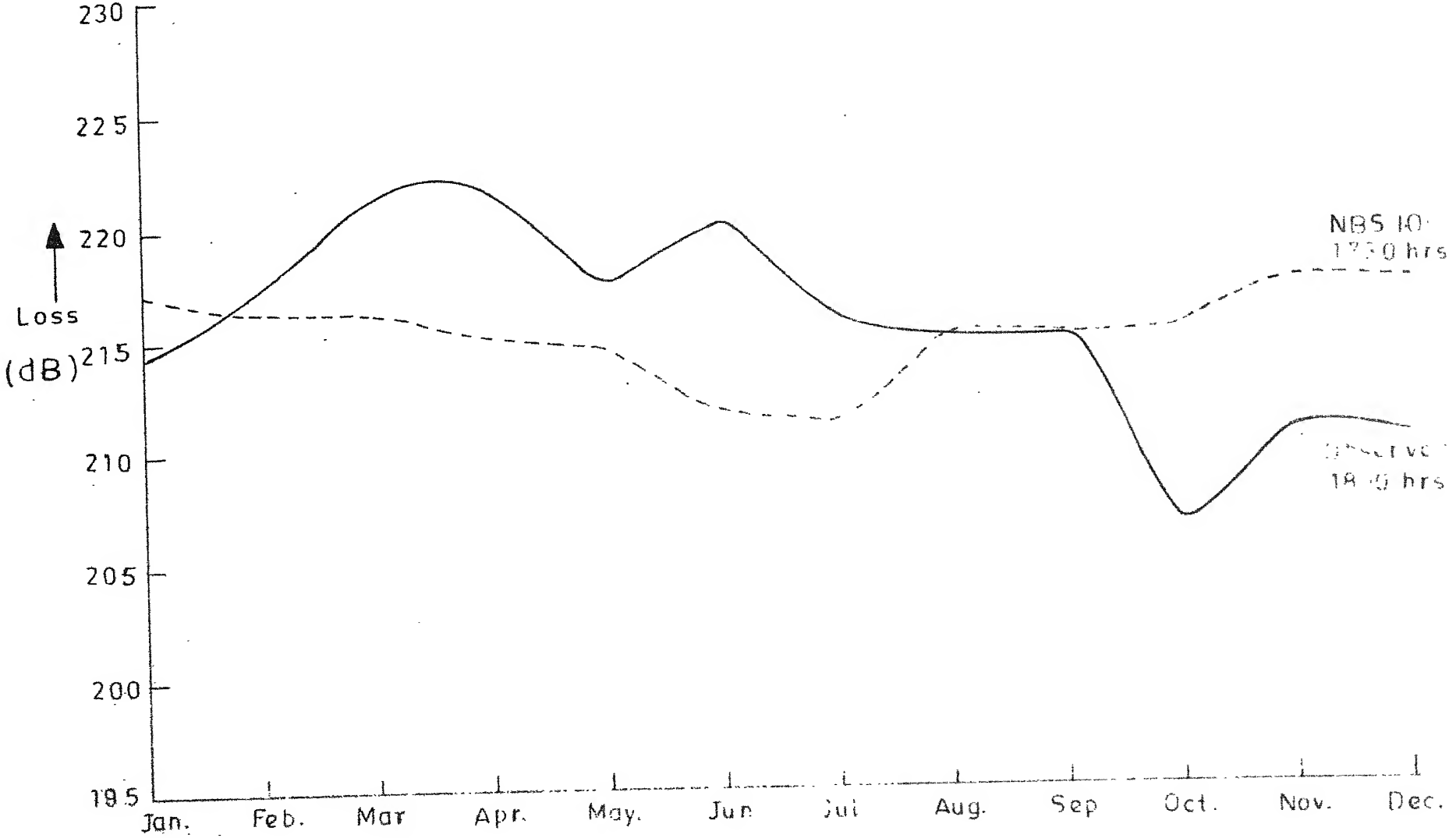

FIG. 6.2 YEARLY DISTRIBUTION OF PATH LOSS AT 0600 hrs AND 1800 hrs. KANPUR-NAINITAL LINK.

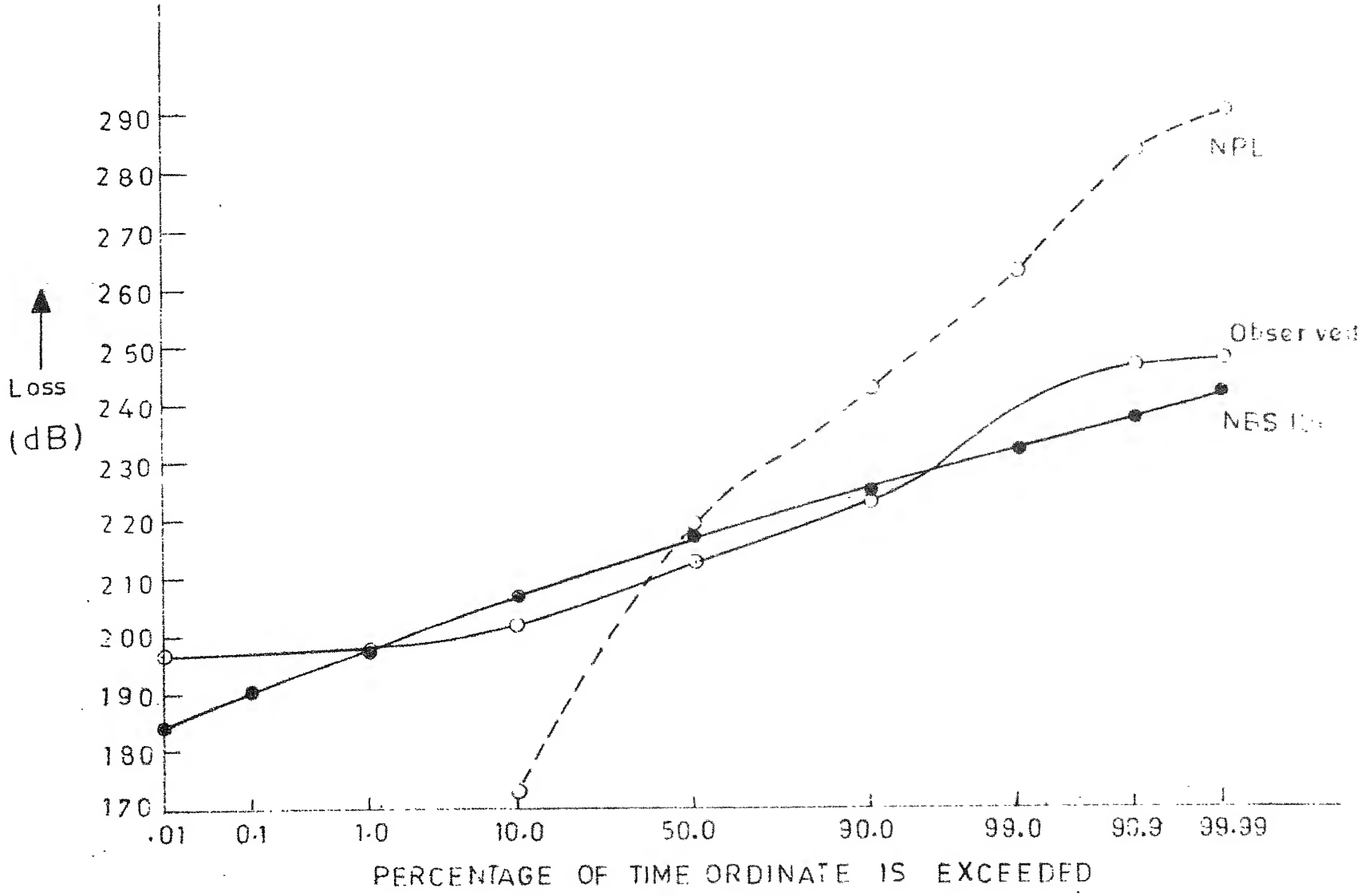

FIG.6.3 CUMULATIVE DISTRIBUTION OF PATH LOSS.
KANPUR – NAINITAL LINK

CHAPTER 7

PATH LOSS SENSITIVITY STUDIES

7.1 Surface Refractivity or Initial Refractivity Gradient

The dependence of path loss on the surface refractivity can be explained as follows. The value of refractive index near the upper boundary of the troposphere remains almost constant with most of the variations of climatic factors, so when surface refractivity, N_s, increases, the gradient of refractivity $\frac{dN}{dh}$ decreases. Dolukhanov[2] gives the simplified expression for the radius of curvature of the ray path as

$$R = \frac{10^6}{\frac{dN}{dh}} \text{ metres} \qquad (7.1)$$

It can be seen that with decrease in $\frac{dN}{dh}$, the radius of curvature of the ray path will decrease, resulting in higher bending and lower scatter angle. Hence the path losses will decrease. Similar arguments can be extended for initial refractivity gradient, ΔN_1, which may be approximated for $\frac{dN}{dh}$ so far as ray bending is concerned.

Studies were conducted to determine the sensitivity to N_s (NBS 101 Method, CCIR Method) and to ΔN_1 (NPL method) of path loss prediction on Kanpur-Nainital link. The sensitivity curves are plotted in Fig. 7.1. The annual range of N_s in the region of this link was found to be varying

from 280 to 400 N-units. In this complete range the NBS 101 method exhibihited a path loss change of only about 10 dBs, indicating that it was not very sensitive to changes in the value of N_s. In the same range of N_s, the CCIR method displayed a path loss range of 65 dBs.

The annual range of ΔN_1 is from -35 to -100 N-units/Km (other than ducting situations). NPL method shows a path loss range of 50 dBs, and is therefore quite sensitive to ΔN_1.

7.2 Scatter Angle

It has been seen in Chapters 3 to 5 that the predicted path loss is dependant on the scatter angle θ. Calculations for various values of θ, extending from 0.5 to 10 degrees, were done for NBS 101, CCIR and NPL models of prediction, for the Kanpur-Nainital link.

The results have been plotted in Fig. 7.2. The NPL method was found to be more sensitive to changes in scatter angle exhibiting a path loss range of about 75 dBs. The behaviour of CCIR model was found to be odd, in that, the path loss was found to decrease with increase in θ. This variation was found to be so due to the empirical curve given in Fig. 5.2 and used in the CCIR prediction method. Beyond this, no logical explanation for this odd behaviour could be given, and it appears to be a basic flaw in the model.

In tropo antennas, it is possible that due to problems of erection or fixing feed horns etc., the elevation angle may not be the planned one, thereby contributing directly to scatter angle of the link. The sensitivity of both these methods in the low scatter angle range can be seen (from Fig. 7.2) to be rather high. Hence any elevation angle errors can change the path loss predictions significantly. For the current scatter angle (as marked in Fig. 7.2), an elevation error of 0.25° will cause a prediction error of approx. 4 dBs for NPL method, and 2.5 dBs for NBS 101 method.

7.3 Effective Earth Radius

It is known that the classical method of accounting for the tropospheric refraction of radio waves is to enlarge the earth's radius to an effective earth radius, and then assume the waves to travel in straight lines. Effective earth radius,

$$a_e = k.a = \frac{a}{1+a\frac{dN}{dh}.10^{-6}} \qquad (7.2)$$

where a is true earth radius (6370 Kms)

k is the effective earth radius factor.

As the effective earth radius factor, k, is increased, we assume that the radius of curvature of the ray is being decreased. Hence there will be more bending, resulting in

smaller scatter angles and, so, less path loss. Calculations of path loss, for various value of k, extending from 1.0 to 2.5, were done for Kanpur-Nainital link, and the results have been plotted in Fig. 7.3. Since k depends on $\frac{dN}{dh}$, the corresponding values of ΔN_1 have also been indicated. CCIR method exhibits a positive change in the value of predicted path loss with increase in k. This abnormal behaviour is again linked to function $k_2(D_s.\theta)$ in Fig. 5.2, due to which the basic path loss increases with decrement of scatter angle θ.

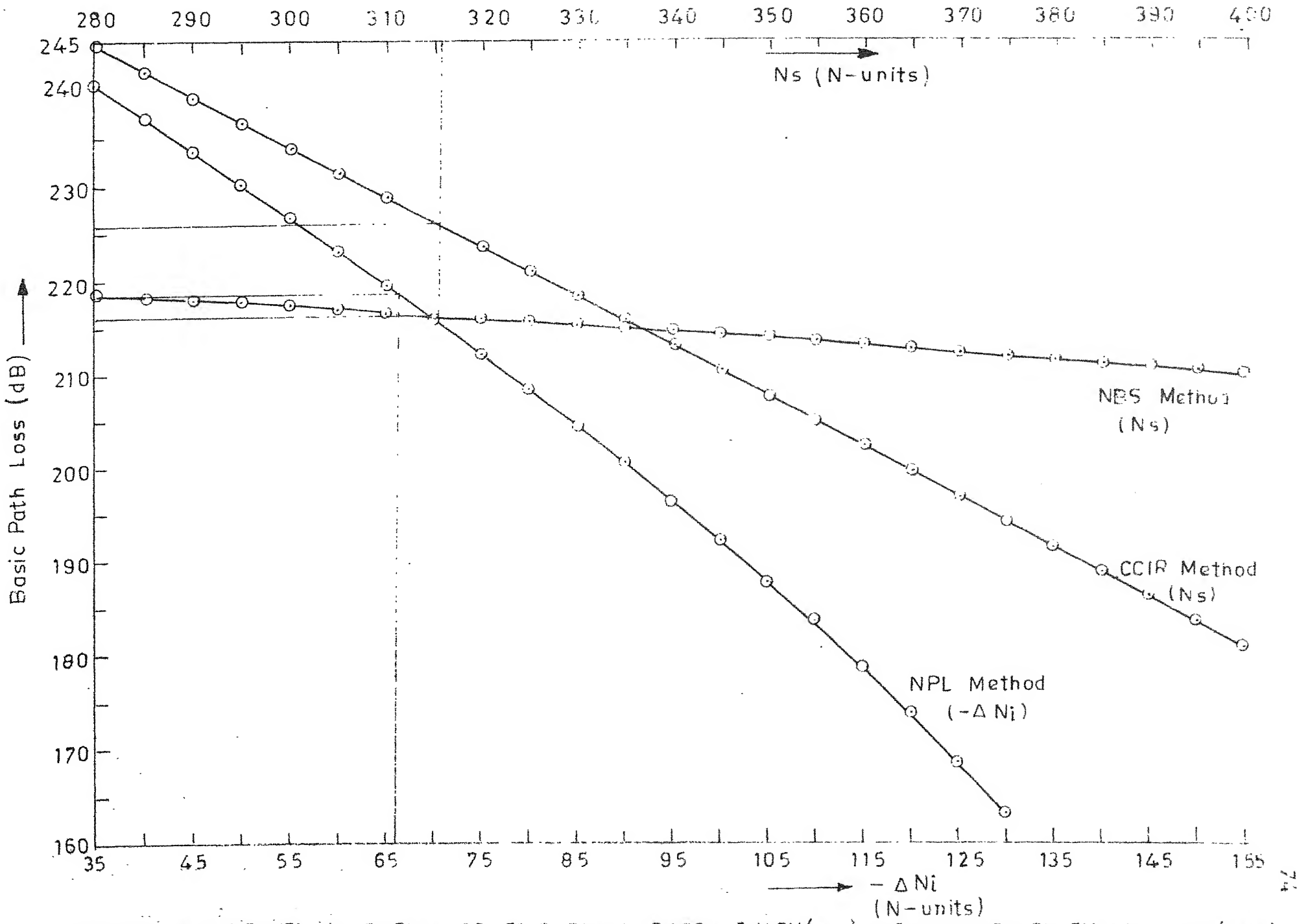

FIG.7.1 SENSITIVITY OF PATH LOSS TO SURFACE REFRACTIVITY(Ns) & INITIAL REFRACTIVITY GRADIENT(Δ Ni)

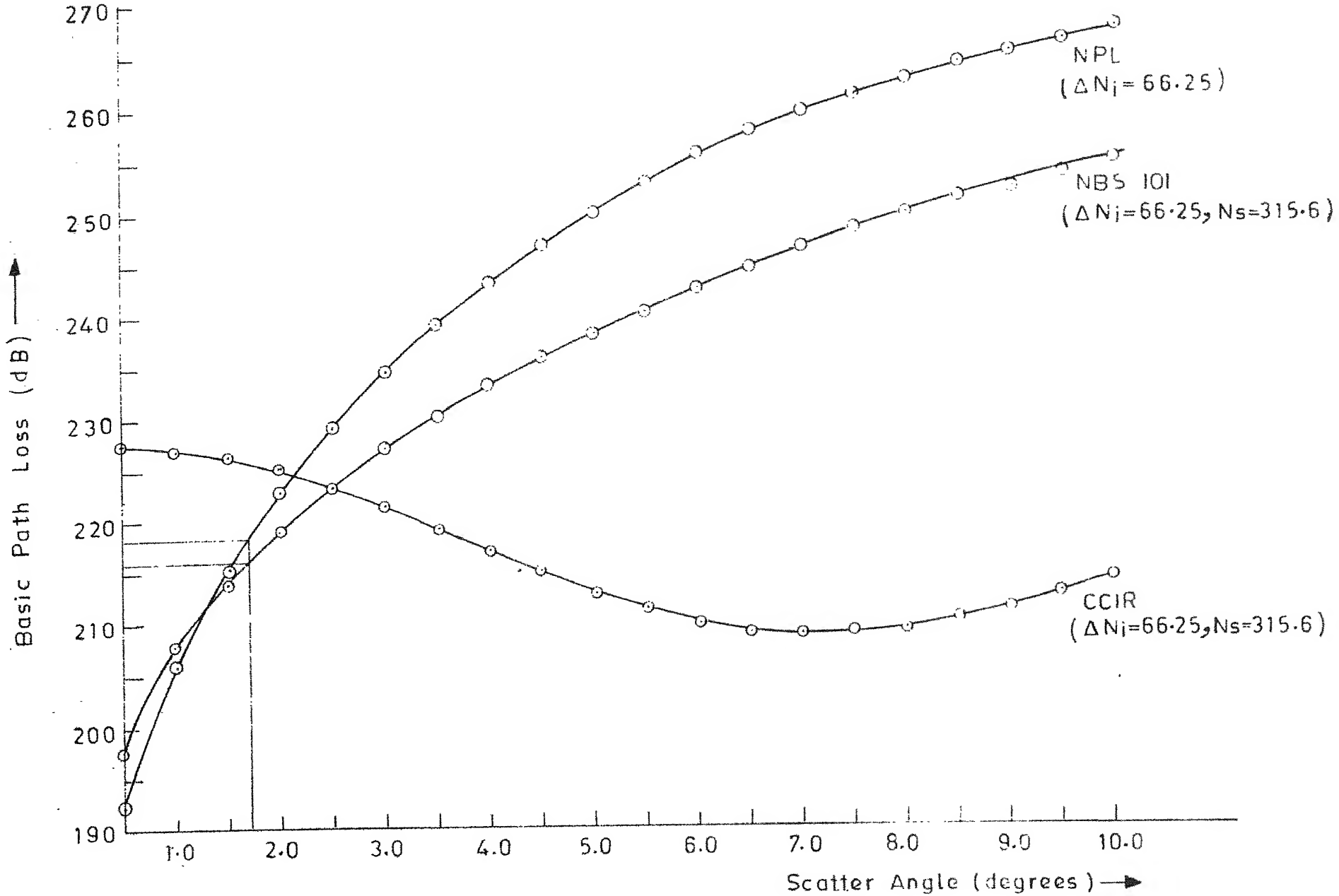

FIG. 7.2 SENSITIVITY OF PATH LOSS TO SCATTER ANGLE

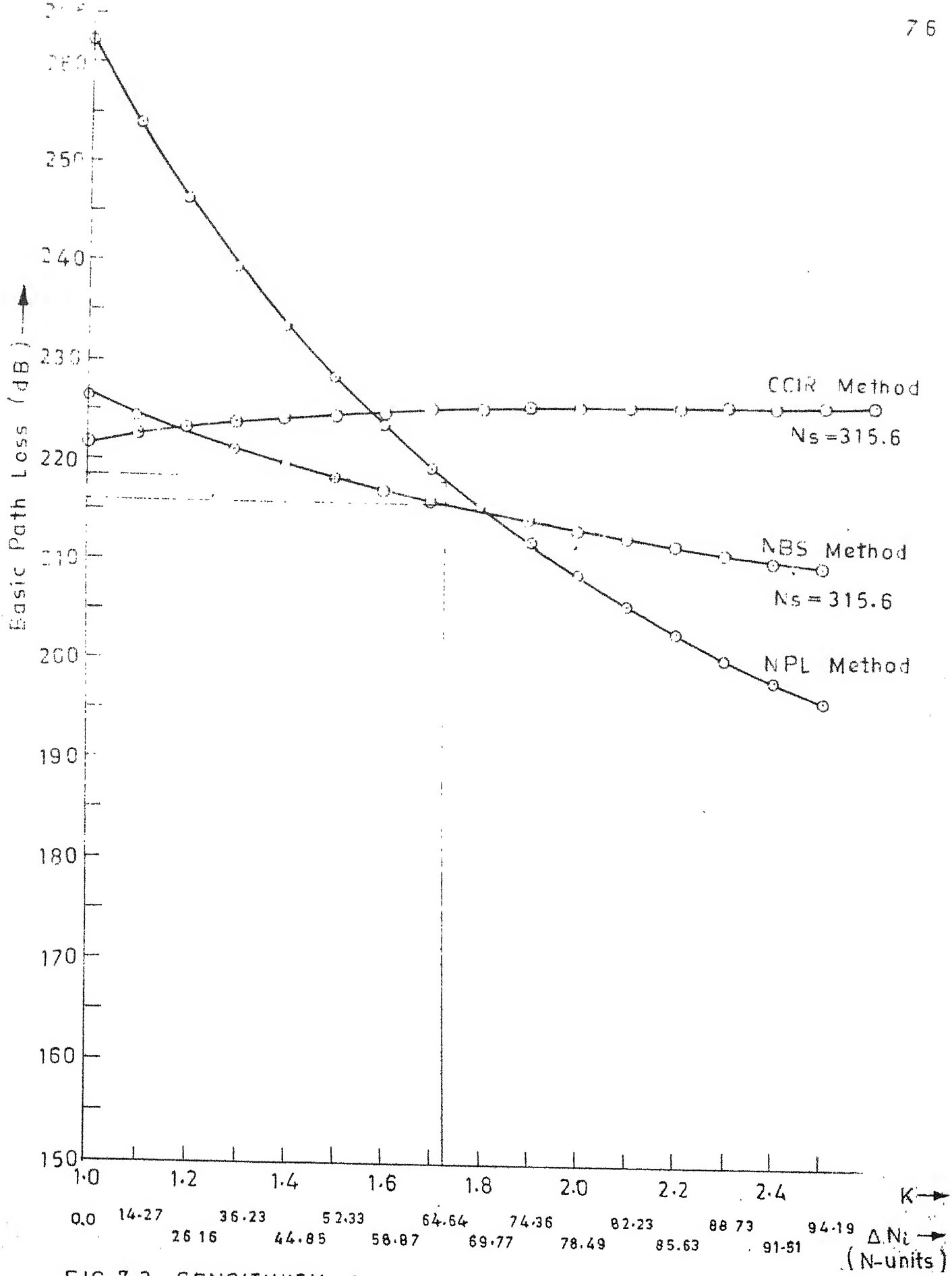

FIG.7.3 SENSITIVITY OF PATH LOSS TO EFFECTIVE EARTH RADIUS FACTOR (K)

CHAPTER 8

EAVESDROPPING AND JAMMING OF TROPOSCATTER LINK

8.1 General

Due to some inherent military advantages of the troposcatter communication system, viz. long distance, suitability over rugged or inhospitable terrain, relatively high degree of security and high propagational reliability on a year-round basis, such systems have become important as one of the military communication channels. Hence, electronic counter measure techniques (ECM) are likely to be adopted to eavesdrop/jam the enemy's link. Since, both, eavesdropping and jamming are related to path losses, an attempt has been made here to evolve a method to predict the path losses for an eavesdropping/jamming terminal. Tewari and Rao[22] have discussed jamming of troposcatter links, assuming the jammer to be located in the great circle plane of the operating link.

A method is given in succeeding sections for finding the path loss between an operating transmitter and an eavesdropper (for various locations of eavesdropper), and between a jammer and its victim receiver (for various locations of jammer) based on NBS 101 model of prediction, as given in NBS 101 vol. II, Annexure III.6. The general case of eavesdropper/jammer located outside the great circle plane of

the operating link has been used, while calculations for the particular case of eavesdropper/jammer being located in the great circle plane have also been done.

8.2 Prediction of Path Losses for an Eavesdropper

For any eavesdropping receiver to be effective, it is necessary that its antenna beam intersect with the operating transmitter beam, and form a common volume with it. Fig. 8.1 gives the geometry for eavesdropping. The operating link TR_1, with a distance d', is assumed to have its beam intersection in the vertical plane Y-Z. The transmitter beam, TP', is assumed to be at an angle ϕ to the horizontal plane X-Y and the line TR_1. An eavesdropping receiver, R_2, is assumed to be located at a distance d from T, in X-Y plane, and deviated at an angle α, in azimuth, to line TR_1. For eavesdropping, the R_2 antenna beam is directed to intersect the antenna beam TP' at any point P, making a scattering angle, θ in the plane TPR_2. Now, assuming that T and R_2 form a troposcatter link and that plane TPR_2 makes an angle γ with the great circle plane containing T and R_2, we can calculate the predicted path loss by NBS 101 method for the case when the antenna beams are directed out of the Great Circle Plane. Angles γ and β give the directions of the antenna beams in the scattering plane TPR_2 for T and R_2 respectively. Angle

is taken to be the elevation of beam R_2P over the horizontal plane X-Y.

In Fig. 8.1, if a perpendicular is dropped from P to TR_2, meeting it at Q', and another perpendicular from P to TR, meeting it at Q, then

$$PQ = TQ \tan \phi, \text{ and } PQ = PQ' \sin\left(\frac{\pi}{2} - \delta\right) \qquad (8.1)$$

where δ is the angle that plane TR_2 makes with the vertical plane at TR_2. From (8.1),

$$TQ \tan \phi = PQ' \cos \delta$$
$$= TP \sin \gamma \cos \delta$$
$$= \frac{TQ}{\cos \phi} \sin \gamma \cos \delta$$

$$\text{or} \quad \cos \delta = \frac{\sin \phi}{\sin \gamma} \qquad (8.2)$$

Taking unit vectors, TP and TR_2, and resolving,

$$\hat{TP} = \cos \phi \ \hat{i}_y + \sin \phi \ \hat{i}_z$$
$$\hat{TR}_2 = \sin \alpha \ \hat{i}_x + \cos \alpha \ \hat{i}_y$$

Taking dot product of these two,

$$\left|\hat{TP}\right| \left|\hat{TR}_2\right| \cos \gamma = \hat{TP} . \hat{TR}_2$$
$$= (\cos \phi \ \hat{i}_y + \sin \phi \ \hat{i}_z).(\sin \alpha \ \hat{i}_x + \cos \alpha \ \hat{i}_y)$$

$$\text{or} \quad \cos \gamma = \cos \phi \cos \alpha \qquad (8.3)$$

In triangle TPR_2, using sine rule,

$$\frac{PR_2}{\sin\gamma} = \frac{PT}{\sin\beta}$$

or $PR_2 = PT \sin\gamma / \sin\beta$

Now, $\sin\delta = \frac{PQ}{PR_2} = \frac{PT \sin\phi}{PT \sin\gamma} \cdot \sin\beta$

or $\sin\delta = \sin\phi \sin\beta / \sin\gamma$ (8.4)

NBS 101 mentions that the path loss for a link, which has its antenna beams directed out of the Great Circle plane, can be calculated by the method given in Chapter 3, but with the following modification. The "scattering plane" is determined by the line between the antenna locations, and the axis of the stronger of the two intersecting beams, making an angle $\mathcal{J}$ with the great circle plane. For effective angles α_e, β_e can be determined as

$$\alpha_{eo} = \alpha_{oo} \sec\mathcal{J} \qquad \beta_{eo} = \beta_{oo} \sec\mathcal{J} \qquad (8.5)$$

Where $\mathcal{J}$ is the angle away from the great circle plane, and α_{oo}, β_{oo} are as defined in Chapter 2, but using the actual earth radius, a_o = 6370 km, instead of an effective earth radius, a_e. Considering the ray bending,

$$\alpha_e = \alpha_{eo} + \tau(\theta_{bt}, \frac{d_{Lt}\sec\mathcal{J}}{2}, N_s) - \tau(\theta_{bt}, \frac{d \sec\mathcal{J}}{2}, N_s) \qquad (8.6)$$

and $$\beta_e = \beta_{eo} + \tau(\theta_{br}, \frac{d_{Lr}\sec\mathcal{J}}{2}, N_s) - \tau(\theta_{br}, \frac{d \sec\mathcal{J}}{2}, N_s) \qquad (8.7)$$

where $\tau(\theta_b, d, N_s)$ is the bending of a radio ray which takes off at an angle θ_b above the horizontal and travels d Kms through an atmosphere characterised by a surface refractivity, N_s. θ_{bt}, θ_{br} are the angles of elevation of the lower half-power point of the antenna beam above the horizontal. The ray bending τ may be determined using methods and tables furnished by Bean and Thayer[26]. For short distances or large angles θ_b, τ is negligible. For a low value of θ_b, we find that the effective earth radius approximation is adequate for determining τ, as follows. Referring to Fig. 8.2, we write the classic expression for bending, following Bean & Thayer[26].

$$d\tau = \frac{-dn}{n} \cot \theta = \frac{-dn}{n} \cdot \frac{dx}{dh}$$

$$\text{or} \quad d\tau = \frac{-1}{n} \cdot \frac{dn}{dh} \cdot dx \qquad (8.8)$$

Finding the total bending,

$$\tau = -\int \frac{1}{n} \frac{dn}{dh} \, dx$$

$$\simeq \frac{-1}{n} \cdot \frac{dn}{dh} \int_0^d dx$$

$$\text{or} \quad = \frac{-1}{n} \cdot \frac{dn}{dh} \cdot d \qquad (8.9)$$

Putting $n \simeq 1$,

$$\tau = -d \cdot \frac{dn}{dh}$$

$$\text{or} \quad \tau = \frac{d}{a_o} \left(1 - \frac{a_o}{a}\right) \qquad (8.10)$$

NBS limits the use of this expression to a θ_b value of 0.1 radians, which would adequately cover most of the tropospheric scatter links.

Now,

$$\theta_e = \alpha_e + \beta_e \quad , \quad s_e = \alpha_e / \beta_e$$

and all further calculations are done by using θ_e and s_e, as given in Chapter 3.

In Fig. 8.1, we can consider the transmitter, T, and receiver, R_2, to be in its great circle plane, but the antenna beams directed out of it. Now plane TPR_2 forms the "scattering plane" and it makes an angle δ with the great circle plane. Since plane X-Y is the horizontal plane joining the two antennas,

(a) α_{oo} (for link TR_1) = ϕ

(b) α_{oo} (for link TR_2) is calculated with actual earth radius a_o

(c) β_{oo} (for link R_2^m) = δ

(d) $\theta_{et} = \theta_{bt}$, $\theta_{er} = \theta_{br}$

Hence, knowing the path geometry, we can find all the essential parameters required to determine the predicted path loss between T and R_2. Assuming an arbitrary eavesdropping receiver, R_2, located on smooth earth at a distance of 300 Kms from T, calculations were made for eavesdropping of Kanpur-Nainital link (with its transmitter at Nainital).

Path loss prediction curves have been drawn, in Fig. 8.3, for azimuthal angle, α, values of 0°, 10° and 30°, and β varying from 1.5° to 10°. Fig. 8.4 gives similar curves, but for α = 5° and distances of 100 Kms, 500 Kms and 1000 Kms. In both the above cases, N_s has been taken to be the Kanpur - Nainital yearly mean value of 315.6 N-units.

8.3 Prediction of Jamming Power for a Jammer

We can consider similar geometry as in Fig. 8.1, but with transmitter, T, replaced by receiver R, and receivers R_1 and R_2 replaced by transmitters T_1 and T_2, where T_1 is the desired transmitter and T_2 is the jamming transmitter. With this, the "scattering plane" remains the same, as in Section 8.2 above, and the same method can be used to predict the path loss between receiver R and jammer T_2.

To jam the receiver effectively, the jamming signal at the receiving antenna should be higher than the desired signal by a certain value. If J is termed as power density of the jamming signal at the receiving antenna, and D as the power density of the desired signal at the receiving antenna, then (J/D) ratio should exceed a certain minimum value. Tewari and Rao[22] have taken this to be 10 dBs. In this thesis also, we assume the same value.

For jamming to be effective for a desired percentage of time, the jammer power must be incremented by a factor M dBs, where M is termed as the jamming reliability factor, or system margin. Considering the worst case situation, that is, when the desired signal is strongest due to least fading, and simultaneously the jamming signal is weakest due to fading, M is defined as

$$M(dB) = L_{fJ} + L_{fd} \tag{8.11}$$

where L_{fJ} is the fade margin for the jamming circuit for the desired reliability, and L_{fd} the fading margin for the desired circuit for the desired reliability. These fade margins can be read from standard curves for varying orders of diversity and reliability. Hence, for a high reliability jammer, factor M will increase, demanding a much higher jamming transmitter power.

The jammer power required now can be calculated as follows.

The power density of the jamming signal at the front end of the receiver will be $(P_J + G_{pJ} - L_J)$ dB where, P_J is the jamming transmitter power in dBs, G_{pJ} is the path antenna gain for the jammer-receiver antennas and L_J is the path loss between the jammer and the receiver.

Similarly, for the desired signal, the power density will be $(P_D + G_{pD} - L_D)$ dB, where P_D, G_{pD} and L_D are the corresponding values for the desired transmitter-receiver link. G_{pD} or G_{pJ} can be determined as follows

$G_{pD(J)} = G_{D(J)} + G_R$ - Antenna-to-Medium Coupling Loss

Curves for determining Antenna-to-Medium Coupling Loss are given in NBS 101.

Now, $P_J = P_D + G_{pD} - G_{pJ} - L_D + L_J + \frac{J}{D} + M$ (8.12)

Sample calculations were done to determine the required jamming power for an arbitrary jammer to jam the Kanpur - Nainital link. Figs. 8.5 and 8.6 give the curves of required Jammer Power vs. β for same variations of distance and azimuth as in the case of eavesdropping. The following jammer parameters have been assumed.

a) Height of jamming transmitter antenna - 800 metres.

b) Effective height of jamming transmitter antenna - 790 metres.

c) All antenna diameters - 8.53 metres (28').

d) Waveguide and Coupling Losses for each link - 4 dB .

e) Jamming reliability factor, M - 10 dBs.

f) Effective Earth Radius - 11021 Kms.

g) Surface Refractivity, N_s - 315.6 N-units.

It is noticed from Figs. 8.5 and 8.6 that jamming a troposcatter link is possible, but only for small distances and small azimuthal variations. For greater distances and azimuthal angles, the power requirements work out to be very high, and may not be easily realizable.

While plotting the curves in Figs. 8.3 to 8.6, function $F(\theta_e d)$ had to be read from NBS 101 vol. II, Fig. III.12, in which $F(\theta d)$ has been plotted against (θd) for various values of s since (θd) has been marked on a logarithmic scale, reading of these curves θ_o give certain inaccuracies. Keeping this in view, the best-eye-fit curves have been drawn.

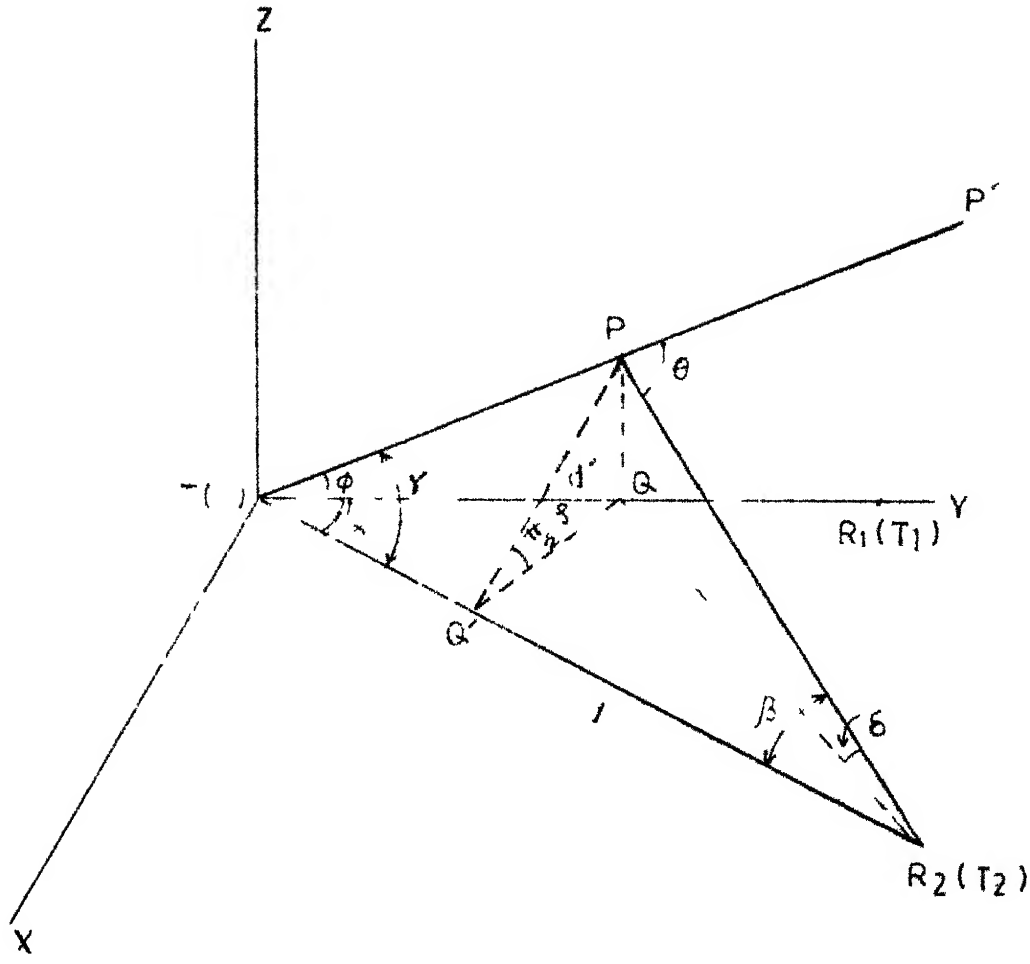

FIG 8 1 GEOMETRY FOR EAVESDROPPING (JAMMING)

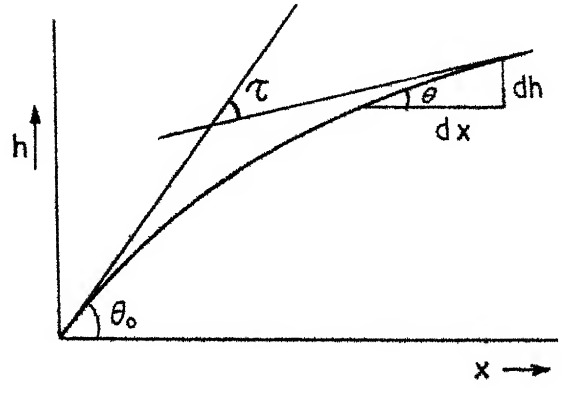

FIG 8 2 BENDING OF RADIO RAY

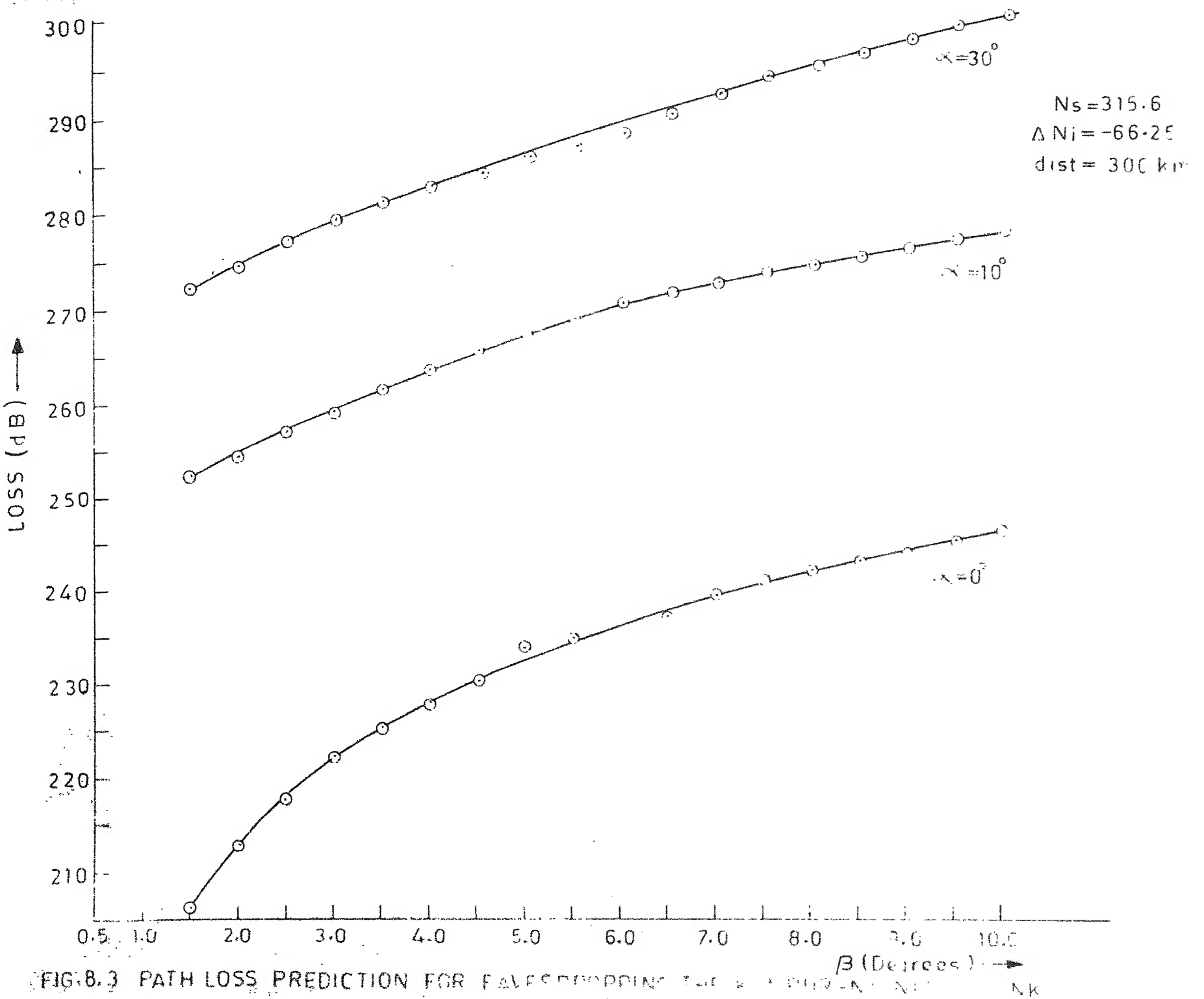

FIG.8.3 PATH LOSS PREDICTION FOR FALLS[illegible]

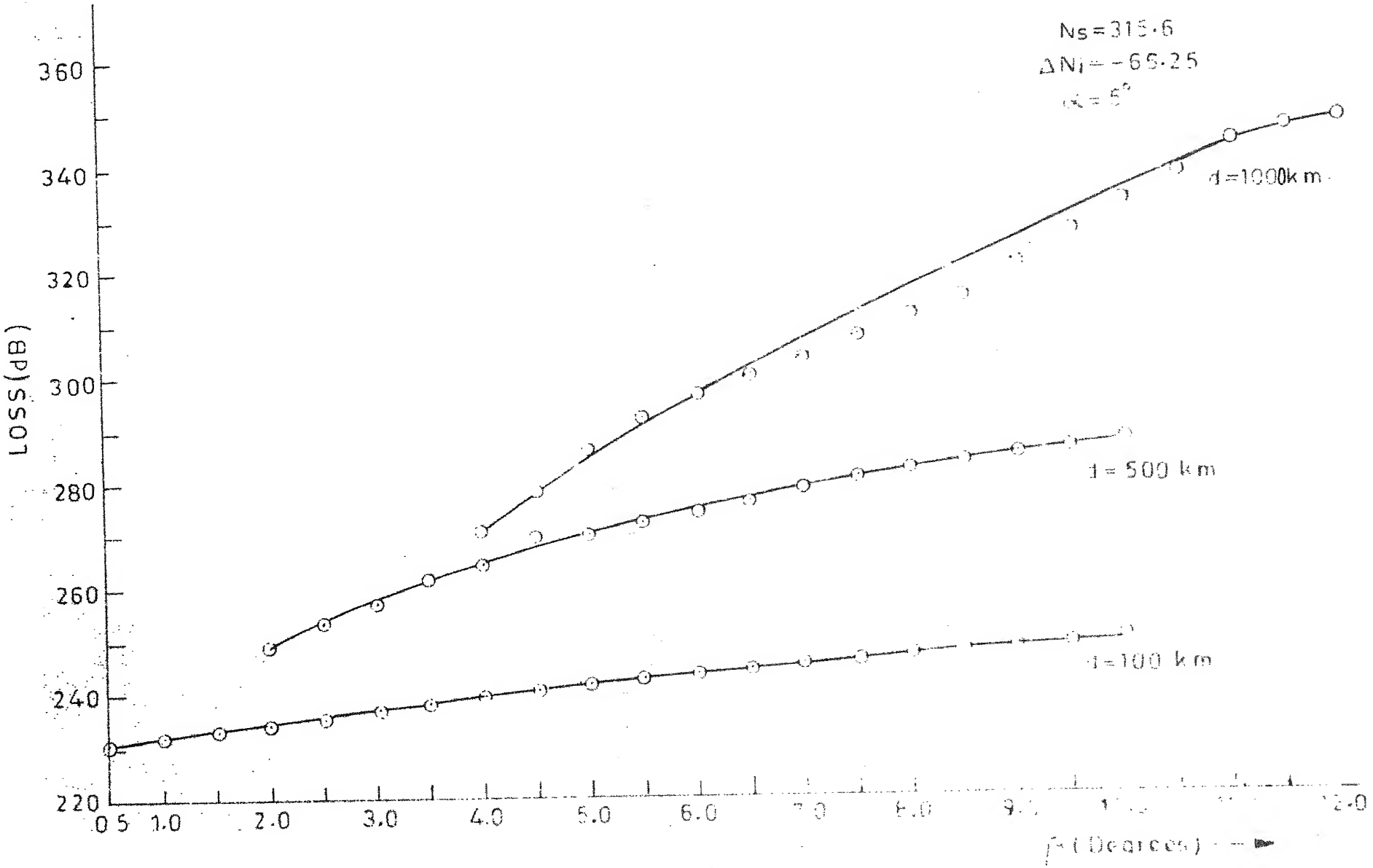

FIG.8.4 PATH LOSS PREDICTION FOR EAVESDROPPING THE KANPUR-NAINITAL LINK

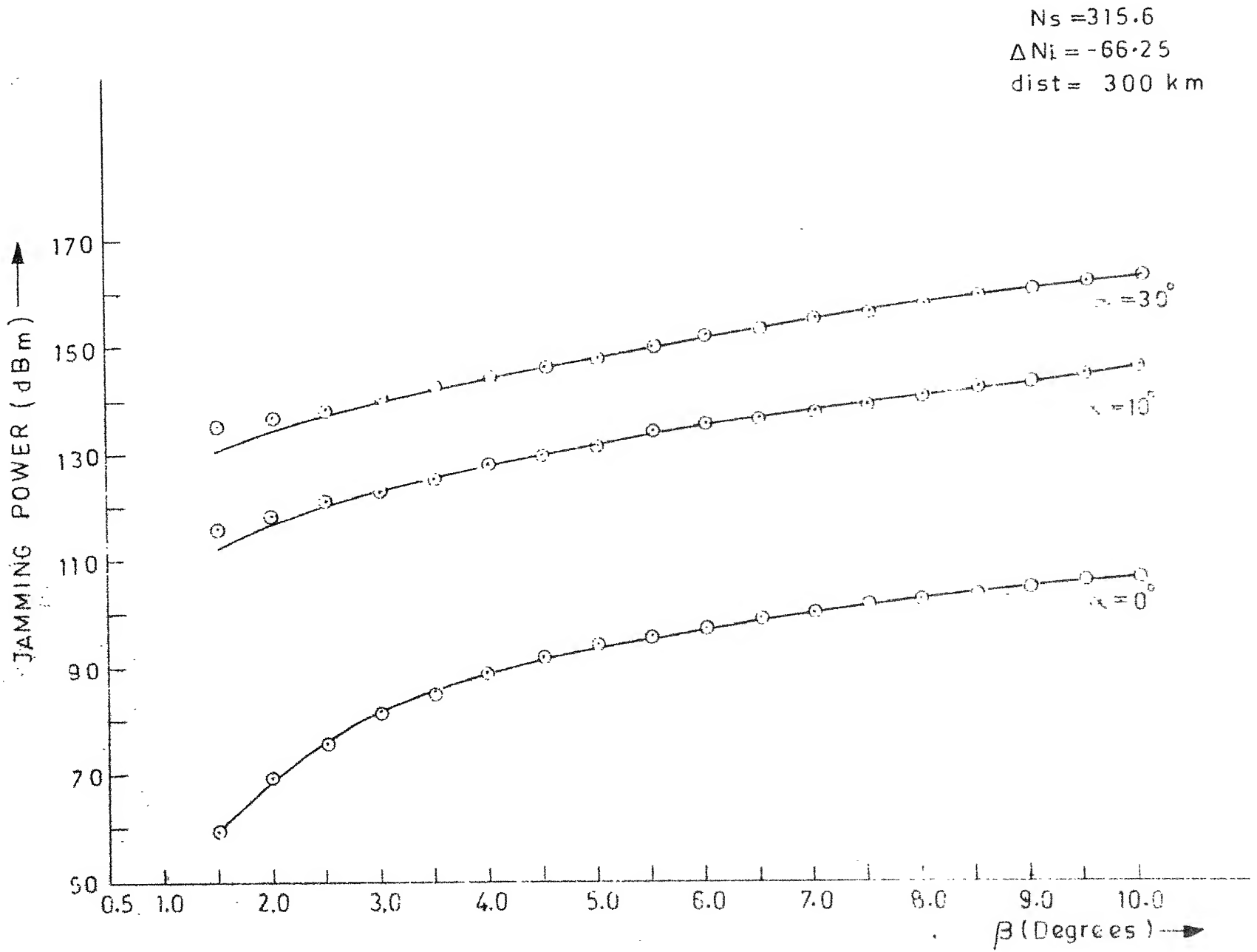

FIG.8.5 JAMMING POWER PREDICTION FOR JAMMING THE KANPUR-NAINITAL LINK

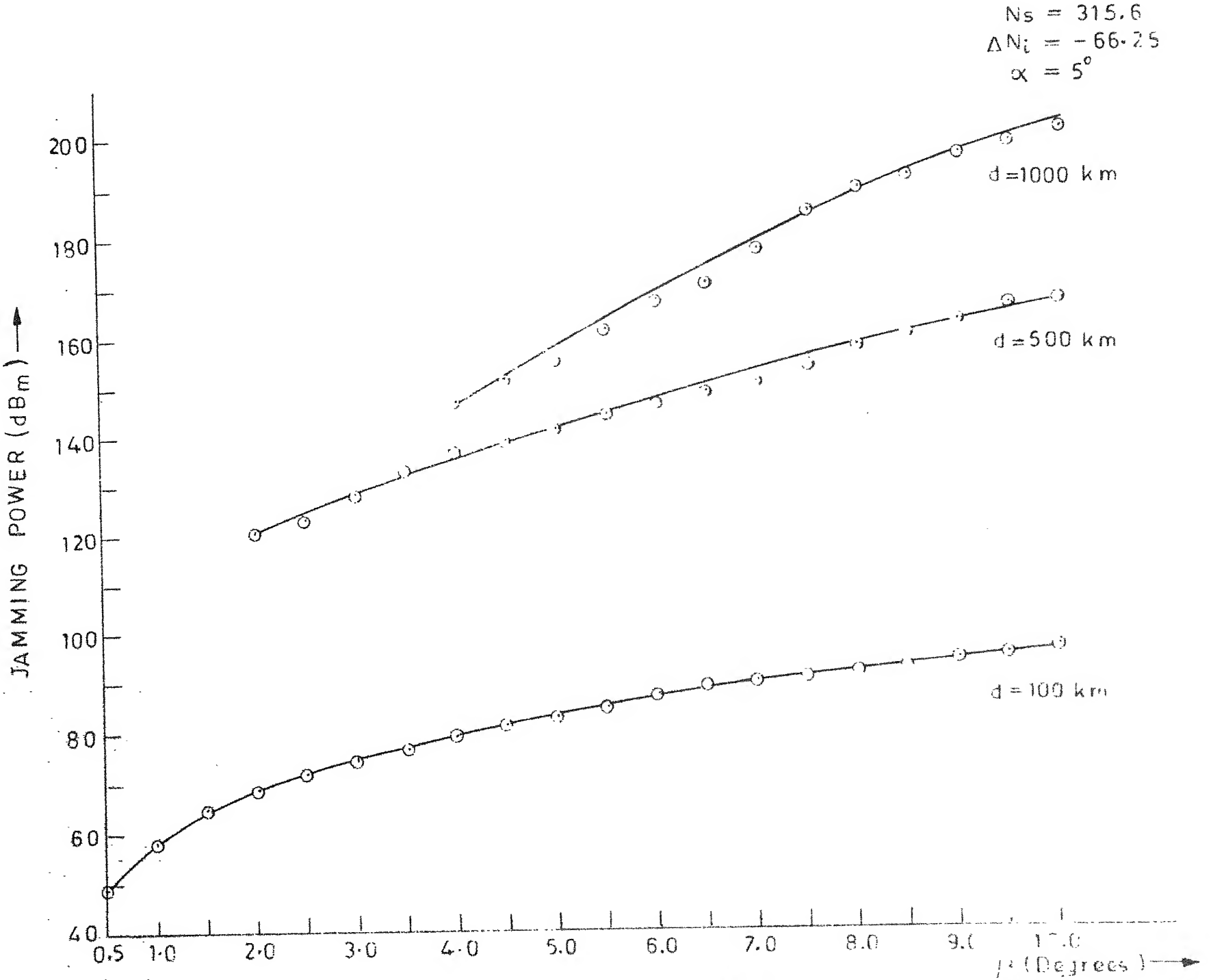

FIG.8.6 JAMMING POWER PREDICTION FOR JAMMING THE KANPUR-NAINITAL LINK

CHAPTER 9

CONCLUSION

The intercomparison of various path loss prediction methods done in Chapter 6 clearly shows that the NBS 101 method, as used by us, correlates better with the observed path loss, for Kanpur-Nainital link. Earlier comparisons made by Majumdar[10,13] and Sarkar[18] over a wide variety of paths, at 120 MHz. and 2 GHz., have revealed the NPL method to be giving more accurate predictions. The above anamoly may be due to the fact that Majumdar and Sarkar, both, may have taken the original model of $\Delta\overline{N}_1$ (for American Conditions) given in NBS 101 for finding the effective earth radius for NBS 101 method, while we have taken $\Delta\overline{N}_1$ (from Atlas) as relevant to the paths. We conclude that NBS 101 method of prediction of path losses may be used for planning purposes, but with a_e calculated from $\Delta\overline{N}_1$, taken from the Atlas. However, more investigation on this comparison needs to be done. Also, currently no method exists to determine the cumulative prediction of path loss for the NPL method. Using available data for various regions, an empirical relationship for predicting path loss for various percentages of time could be evolved.

Since the odd behaviour of CCIR (French Administration) method, with respect to the scatter angle could not be resolved, it is suggested that this method not be used any more. Parl's method appears to be very general, and studies could be carried out to try and fit a value to slope, m, for various regions of the country, based on comparison of predicted results and observed data. This method could not be investigated, in details, here since it could be made available very recently.

Sensitivity of path loss calculations to $N_s/\Delta N_1$, and scatter angle, revealed the extent of error that could be expected when we are either using unsure data ($N_s/\Delta N_1$) or when there has been certain misalignment or errors in erection of antennas (causing change in the scatter angle).

Studies on jamming and eavesdropping of troposcatter communication links showed that given Electronic Support Measures (ESM), it is possible to conduct Electronic Warfare on a 'tropo' link, even when the hostile receiver or transmitter is not in the great circle plane of the existing link. In addition, since the received signal level (for eavesdropping), and the required jamming power (for jamming),

can actually be predicted, both these operations can be fully planned. It would, perhaps, be worthwhile to experimentally try eavesdropping/jamming by mobile tropo equipment, to determine the accuracy of these predictions.

REFERENCES

1. CCIR, XIII Plenary Assembly, Geneva, 1974, Vol. V, Reports 233-3, 238-2, 425-1.

2. Dolukhanov, M., 'Propagation of Radio Waves', MIR Publishers, Moscow, 1971.

3. DuCastel, F., 'Tropospheric Radio wave Propagation Beyond the Horizon', Permagon Press, London, 1966.

4. Eklund, F. and Wickerts, S., 'Wavelength Dependence of Microwave Propagation Far Beyond the Radio Horizon', Radio Science 3(11), November, 1968, p. 1066.

5. Friis, H.T., Crawford, A.B. and Hogg, D.C., 'A Reflection Theory for Propagation Beyond the Horizon', BSTJ Vol. 36, May,1957, p. 627.

6. Gupta, G.C., 'Tropospheric Probing by Scatter Communications', M.Tech. Thesis (1973), IIT, Kanpur.

7. Gordon, W.E., 'Radio Scattering in the Troposphere', Proc. IRE 43, Jan. 1955, p. 23.

8. Larsen, R., 'A Comparison of Some Troposcatter Prediction, Methods', Conference on Tropospheric Wave Propagation, IEE, London, 30 Sep.-02 Oct.,1968, p. 110.

9. Longley, A.G. and Rice, P.L., 'Prediction of Tropospheric Radio Transmission Loss Over Irregular Terrain - A Computer Method - 1968', ESSA Technical Report ERL 79 - ITS 67.

10. Majumdar, S.C., 'Transhorizon Tropospheric Propagation Studies over the Indian Subcontinent', Centre of Research on Troposphere, NPL, Report, CENTROP-13, March,1974.

11. Majumdar, S.C., Raina, M.K. and Sarkar, S.K., 'Reference Data Manual', Centre of Research on Troposphere, NPL, Report CENTROP-8, Aug.1973.

12. Majumdar, S.C., Sarkar, S.K. and Mitra, A.P., 'Atlas of Tropospheric Radio Refractivity Over the Indian Subcontinent', NPL, 1977.

13. Majumdar, S.C., 'Prediction of Transmission Loss Over Transhorizon Tropospheric Propagation Paths in the Indian Subcontinent', Indian Journal of Radio and Space Physics, Vol. 5, p. 152.

14. Mitra, A.P., Reddy, B.M. and Agarwal, S., 'Tropospheric Propagation and Antenna Measurements', NPL, 1975, Printed by INSDOC.

15. Pande, P.R., 'Qualitative and Quantitative Study of Signal Behaviour for Kanpur-Nainital Troposcatter Link', M.Tech. Thesis (1977), IIT, Kanpur.

16. Parl, S.A., 'New Formulas for Tropospheric Path Loss', Radio Science 14(1), Jan. 1979, p. 49.

17. Rice, P.L., Longley, A.G. and others, 'Transmission Loss Predictions for Tropospheric Communication Circuits', NBS 101, Vols. I & II, May, 1965 and May,1966.

18. Sarkar, S.K., 'Radioclimatological Effects on Tropospheric Radiowaves Propagation Over the Indian Subcontinent', Centre of Research on Troposphere, NPL, Report CENTROP-32, Aug.,1978.

19. Tatarski, V.I., 'Wave Propagation in a Turbulent Medium', McGraw Hill Book Co. Inc., New York, 1961.

20. Tatarski, V.I., 'The Effects of the Turbulent Atmosphere on Wave Propagation', Israel Program for Scientific Translation, Jerusalem, 1971.

21. Thayer, G.D., 'Radio Reflectivity of Tropospheric Layers', Radio Science 5(11), Nov. 1970, p. 1293.

22. Tewari, R.K. and Rao, E.B., 'Jamming Vulnerability of Tropo Links', Journal Institution Telecom. Engrs., 19(1), Jan. 1973.

23. U.S.A.E.P.G. - SIG960-67, 'Instruction Manual for Tropospheric Scatter - Principles and Applications', U.S. Army Electronic Proving Ground, Fort Huachuca, Arizona, March,1960.

24. Venkiteswaran, S.P. and V.S. Narayanan, RTRC Monograph Nos. 1 and 2, NPL, 1970-1972.

25. Wait, J.R., 'Electromagnetic Waves in Stratified Media', Permagon Press, London, 1962.

26. Bean, B.R. and Thayer, G.D., 'Models of the Atmospheric Radio Refractive Index', Proc. IRE, May,1959.

27. Girdhar, V.K., 'A Study of the Relationship of Troposcatter Path Loss with Meteorological Parameters', M.Tech. Thesis (1979), IIT Kanpur.

A59546